SOME FEATURES OF VELOCITY DISTRIBUTIONS OF TURBULENT FLOWS OF AN INCOMPRESSIBLE FLUID IN BOUNDARY LAYERS AND IN CHANNELS

OKABE, Jun-ichi
Research Institute for Applied Mechanics, Kyushu University

https://doi.org/10.5109/7165056

出版情報：Reports of Research Institute for Applied Mechanics. 12 (44), pp.71-107, 1964. 九州大学応用力学研究所
バージョン：
権利関係：

Reports of Research Institute for Applied Mechanics
Vol. XII, No. 44, 1964

SOME FEATURES OF VELOCITY DISTRIBUTIONS OF TURBULENT FLOWS OF AN INCOMPRESSIBLE FLUID IN BOUNDARY LAYERS AND IN CHANNELS

By Jun-ichi OKABE

Summary

Phenomenological studies are outlined concerning some features of velocity distributions of turbulent flows of an incompressible fluid in boundary layers and in channels. Turbulence is assumed steady on its time-average and effect of roughness of walls is ignored altogether. Unless otherwise explicitly stated, in the following sections fluid motions are assumed completely turbulent.

Section 1 is devoted to introduction of the paper.

In **section 2**, velocity defects are defined both for boundary layers and channel flows. It is clarified that in contrast with the former in which a sharp trough can be found, depression in the latter is not well-defined.

Accuracy of the power law asserted by LUDWIEG and TILLMANN for the distribution of velocity near the wall is examined in **section 3**. It is observed to hold good more accurately in boundary layers than in channel flows.

Section 4 is concerned with so-called PRETSCH's formula for velocity profiles. It is sufficiently verified by virtue of the experimental data obtained for boundary layers and channel flows.

The object for study in **section 5** is turbulent shearing stress in channel flows. By applying the computation invented by FEDIAEVSKY for boundary layers the following conclusions are derived: i) In channel flows polynomial method provides adequate approximation for the distribution of shearing stress in the cases α (one half of the angle of divergence) $= 0°$ (parallel walls) and $\alpha = 4°$ (substantially the limit up to which symmetry of flow can be maintained) and that, however, at angles intermediate between them the accuracy is rather insufficient. ii) For a converging channel (α negative) agreement with experiments is extremely poor.

The content of **section 6** is a brief discussion on the assumption which was introduced by BURI and HOWARTH. Namely with a special view to establishing an approximate method of treatment of boundary layers, they put H and ζ, the form parameter of velocity profiles and the coefficient of skin friction respectively, in the same functional forms of a single variable Γ as obtained experimentally in channel flows. However, analyzing the computations performed by VON DOENHOFF and TETERVIN for the boundary layer of an airfoil on the one hand together with the empirical results obtained by SCHUBAUER and KLEBANOFF using an airfoil-like section placed in a wind tunnel on the other, the functions $H(\Gamma)$ and $\zeta(\Gamma)$ are both revealed to become *two-valued* near the separation point of boundary layers, in so far as these examples are concerned.

Finally, for velocity profiles in laminar boundary layers, similar accounts are given in the **appendix** on velocity defects, LUDWIEG-TILLMANN's law and PRETSCH's formula.

1. Introduction

In computing a turbulent boundary layer formed on a surface of an obstacle submerged in a uniform stream of an incompressible fluid, analogies with a flow in a pipe or in a channel have been employed, sometimes quite successfully.[1] For example, velocity distributions across sections of the boundary layer formed along a flat plate may be approximated within a certain range of REYNOLDS numbers very closely by the so-called '1/7th power law' due to BLASIUS. It is well-known, however, that this law is, in fact, a semi-empirical formula derived for flows in pipes.[2] Nevertheless, it has to be realized distinctly that the degree of hydrodynamical constraint upon friction layers is much different between flows in boundary layers and those in pipes and channels. Namely, in the former only one side of the flow field otherwise extending to infinity is bounded by a solid surface, while in the latter vortices originated from the wall lying on the opposite side of the channel may be transferred freely across the central axis and finally steady field of turbulence is established downstream.

Let us take the x-, and the y-, axes along and perpendicularly to the surface of a body, respectively. Denoting the displacement, and the momentum, thicknesses of the boundary layer along the surface of the body by $\delta_1(x)$ and $\vartheta(x)$, the x-, and the y-, components of the mean velocity by u and v, respectively,[3] and further the value of u on the outer edge of the boundary layer ($y = \delta$) by u_1, it was pointed out by VON DOENHOFF and TETERVIN that the velocity profile, u/u_1, or the distribution of velocity across sections, of boundary layers accompanied by various pressure gradients along streamlines, is expressed as a function of the variable $H \equiv \delta_1/\vartheta$ for a given value of the non-dimensional distance y/ϑ.[4] This conclusion is very important, because it means that boundary layer profiles form a single-parameter family of curves. By examining, therefore, whether or not this

1) In the following sections, the effect of roughness is always left out of consideration. In other words, surfaces of submerged obstacles, walls of pipes and of channels are all assumed to be smooth hydrodynamically. Further, unless otherwise explicitly stated, assumptions are made concerning flow behaviors that in all cases they are completely 'turbulent' and 'quasi-steady' which means steady on the average taken with respect to time. When, therefore, we mention simply 'boundary layers' or 'channel flows', we mean 'turbulent boundary layers' or 'turbulent flows in channels' respectively, whose conditions may be regarded as quasi-steady. Laminar boundary layers will be touched upon in the appendix at the end of the paper.

2) GOLDSTEIN, S., *Modern Developments in Fluid Dynamics*, vol. II (1938), **163**, p. 361 *et seq.*

3) Average is taken always with regard to time. In the following discussions concerning fluctuating quantities, the adjective 'mean' will be usually omitted for simplicity.

4) VON DOENHOFF, A. E. and TETERVIN, N., Determination of General Relations for the Behavior of Turbulent Boundary Layers, *NACA Technical Report* 772 (1943), esp. FIGS. 9 and 10, pp. 12 and 13.

functional relation should remain valid also for flows in pipes or channels, diverging or converging, we should be able to find some clues to full understanding of features of velocity distributions in boundary layers and in pipes or channels. This was performed in practice by HAYASHI making use of the experimental data due to NIKURADSE.[1)2)] The results obtained are embodied in *FIGURE 1* of his paper,[3)] and the conclusions were summarized as follows:

i) The fundamental property that u/u_1 be expressed as a function of y/ϑ and H is preserved invariably for flows in channels.[4)]

ii) But the relationship shows some discrepancy from that obtained by VON DOENHOFF and TETERVIN for velocity profiles in boundary layers.

iii) Therefore, when we are going to apply experimental results measured for flows in diverging or converging channels directly to boundary layers with pressure gradients, positive and negative respectively along streamlines, we must expect error of order of this discrepancy, at least, to be inevitable.

As an extension of HAYASHI's study, this note has an object of comparing in more detail some features of velocity distributions in boundary layers and in channels. In section 2, from the data of measurements of velocity profiles, 'velocity defects' D_{tb} (turbulent boundary layers) and D_c (channels) defined respectively by (2.1) and (2.2) are evaluated. It is clarified that although D_{tb} exhibits a sharp trough in the range $y/\vartheta < 1$, each of curves of D_c has a depression, not so distinct nor so large as the former.

The accuracy of the power law (3.1) asserted by LUDWIEG and TILLMANN for the distribution of velocity near the wall is examined in section 3,[5)] and the law is found to be valid approximately. Only, it is observed to hold good more

---

1) HAYASHI, M., A Remark Concerning the Experiment by NIKURADSE (in Japanese), *Technology Reports of the Kyushu University*, vol. 27, no. 1 (1954), pp. 7–8.

2) NIKURADSE, J., Untersuchungen über die Strömungen des Wassers in Konvergenten und Divergenten Kanälen, *Forschungsarbeiten auf dem Gebiete des Ingenieurwesens*, Heft 289 (1929), or GOLDSTEIN, S., *op. cit.*, **166**, p. 371 *et seq.*

3) In order to avoid confusions, figures and tables quoted from references are printed in *italic*, and those belonging to this note in roman, letters.

4) At this point the present writer would like to touch on his own paper 'Note on an Experiment by G. S. BAKER (1930)' (in Japanese), *Bulletin of Research Institute for Applied Mechanics*, no. 3 (1953), pp. 58–60, where by analyzing BAKER's experimental data of velocity profiles on the hull of a ship, the relation existing, if any, among the quantities u/u_1, y/ϑ, and H is examined in detail (BAKER measured six profiles in rough and calm weathers). In cases of rough weather, sea is naturally imagined filled up with vortices of miscellaneous extent and intensity, and so in the boundary layer of a ship, there are certainly contained 'sea vortices', invading from outside and independent of the scale of those turbulence elements which originate from the boundary layer itself. After some computations, however, it was proved that i) u/u_1 may be still regarded as a function of y/ϑ and H, and that moreover ii) its functional form may be expressed approximately by the extrapolations of curves given by VON DOENHOFF and TETERVIN. These facts are supposed to have some bearings with the flow property, just described, in channels.

5) LUDWIEG, H. und TILLMANN, W., Untersuchungen über die Wandschubspannung in Turbulenten Reibungsschichten, *Ingenieur-Archiv*, Bd. 17 (1949), S. 288–299, bes. Abb. 1, S. 290.

accurately in boundary layers than in channel flows.

Section 4 is concerned with the correlation between γ, a new parameter defined by (4.1), and H, the form parameter used hitherto to characterize velocity profiles. It is shown that the formula (4.8) derived by assuming a power law for velocity profiles coincides practically with the relationship obtained from measurements both in boundary layers (VON DOENHOFF and TETERVIN, *op. cit.*) and in channels (NIKURADSE, *op. cit.*). (The content of this section is a well-known fact and adds nothing new to our knowledges of behaviors of friction layers.)[1]

The object for study in section 5 is the distribution of turbulent shearing stress. The computation first invented by FEDIAEVSKY for boundary layers is adapted to flows in channels,[2] and the following conclusions are derived through comparing the theoretical result with the experiment by NIKURADSE. i) Corresponding to the facts that in boundary layers agreement between the polynomial representation for shearing stress and the values obtained from measurement is fairly good in the neighborhood of the points of the minimum pressure and of separation, and that, however, at points intermediate between them discrepancy is quite large,[3] it is shown similarly that in channel flows satisfactory approximation is provided both for the cases α (one half of the angle of divergence) $= 0°$ (parallel walls) and $\alpha = 4°$ (substantially the limit up to which symmetry of flow can be maintained) and that at angles intermediate between them the theory is not adequate. ii) For a converging channel (a negative α, in other words), agreement between the mathematical expression and the observation is extremely poor.

The content of section 6 is a brief discussion on the assumption introduced by BURI and HOWARTH with a special view to establishing an approximate treatment of boundary layers.[4][5] Namely, out of empirical data obtained in channel flows, they assumed analogically that flow behaviors in boundary layers, specifically the form parameter H as well as the non-dimensional friction ζ defined by (6.2), would be functions of Γ alone, which is another variable defined in (6.3). Analyzing the computational result worked out by VON DOENHOFF and TETERVIN (*ibid.*) for the boundary layer along an airfoil on the one hand, together with the empirical result obtained by SCHUBAUER and KLEBANOFF (*ibid.*) using an airfoil-like section placed in a wind tunnel on the other, it is noticed that in so far as these examples are concerned the functions $H(\Gamma)$ and $\zeta(\Gamma)$ are found to be-

1) GRANVILLE, P. S., A Method for the Calculation of the Turbulent Boundary Layer in a Pressure Gradient, *The David Taylor Model Basin Report* 752 (1951), esp. eq. [42], p. 19.

2) FEDIAEVSKY, K., Turbulent Boundary Layer of an Aerofoil, *Journal of the Aeronautical Sciences*, vol. 4 (1937), no. 12, pp. 491-498.

3) SCHUBAUER, G. B. and KLEBANOFF, P. S., Investigation of Separation of the Turbulent Boundary Layer, *NACA Technical Report* 1030 (1951), esp. p. 8.

4) BURI, A., Eine Berechnungsgrundlage für die Turbulente Grenzschicht bei Beschleunigter und Verzögerter Strömung, *Zürich Dissertation* (1931).

5) HOWARTH, L., The Theoretical Determination of the Lift Coefficient for a Thin Elliptic Cylinder, *Proceedings of the Royal Society*, A, vol. 149 (1935), pp. 558-586, esp. 574-579. GOLDSTEIN, S., *op. cit.*, **194**, p. 436 *et seq.*

come *two-valued* near the point of separation. It is suggested from these tests that closer investigations might be necessary for establishing general validity of their assumption.

Finally in the appendix, for laminar boundary layers, velocity defect D_{lb} defined by (A.5) is computed. It is shown also that LUDWIEG-TILLMANN's law for velocity profiles holds good approximately just as for turbulent boundary layers. It is quite interesting to note that, except the separating velocity profile, PRETSCH's formula is still valid which was verified for turbulent flows in boundary layers and in channels.

The writer is very grateful to Messrs. S. INOUE, H. AOKI, and N. FUKAMACHI, and Miss S. HOSHINO for assistances in preparing the manuscript.

2. Velocity defects

By *FIGURE 10* of their paper (see footnote 4, p. 72), VON DOENHOFF and TETERVIN showed the relationship between u/u_1, non-dimensional velocity distribution across sections of the boundary layer, and y/ϑ, non-dimensional distance from the surface, with the aid of the auxiliary variable H, the form parameter defined by the ratio δ_1/ϑ. The fact is that these curves were drawn by plotting points inversely from the family of curves of *FIGURE 9* which expresses u/u_1 as a function of H, containing y/ϑ as a parameter. 'The data presented in figure 9 represent the collection of all the boundary-layer profiles that enter into the analysis',[1] and so *FIGURE 10* produced from it is supposed to have the accuracy almost comparable. The parameter H appearing in *FIGURE 10* takes 15 kinds of values from 1.286 through 2.7,[2] and choosing 8 curves out of them (namely $H=1.286$, 1.5, 1.7, 1.9, 2.1, 2.3, 2.5, and 2.7), values of u/u_1 are read for various values of y/ϑ at intervals of 0.1. Subtracting from a value of u/u_1 corresponding to a pair of H and y/ϑ, that derived by varying H to 1.286 while keeping y/ϑ unchanged, we shall call the difference the 'velocity defect' in the boundary layer, denoting it by D_{tb} (*tb* refers to turbulent boundary layers).[3] Namely the velocity defect for those values of H and y/ϑ such that $H=H_*$ and $y/\vartheta=y_*/\vartheta$ is given by the formula

$$D_{tb} \equiv \frac{u}{u_1}\left(H_*, \frac{y_*}{\vartheta}\right) - \frac{u}{u_1}\left(1.286, \frac{y_*}{\vartheta}\right) \tag{2.1}$$

1) VON DOENHOFF, A. E. and TETERVIN, N., *ibid.*, p. 11. However, profiles corresponding to accelerated main flows are not included in their figures.

2) $H=1.286=9/7$. This value of H can be easily derived from its definition by assuming the 1/7th power law for the velocity profile, and so corresponds to the flow along a flat plate. According to VON DOENHOFF and TETERVIN, 'Separation has not been observed for a value of H less than 1.8 and appears definitely to have occurred for a value of H of 2.6. Gruschwitz's criterion for imminent separation is equivalent to a value of H of 1.85' (*ibid.*, p. 11).

3) This definition was suggested for the first time by ROSS and ROBERTSON for flows in channels. Linearity of curves of the velocity defect in the region of large y was remarked by the original authors; cf. ROSS, D. and ROBERTSON, J. M., A Superposition Analysis of the Turbulent Boundary Layer in an Adverse Pressure Gradient, *Journal of Applied Mechanics*, vol. 18 (1951), no. 1, pp. 95-100, esp. 97. Also see eq. (2.2) to appear.

in the boundary layer. Next, in the paper by NIKURADSE concerning the experiments in diverging and converging channels (see footnote 2 on p. 73), u/u_0 is shown in *ABBILDUNG 10* (S. 19) as a function of y/b, u_0 being the velocity of stream at the center of the channel (the maximum speed, in other words), y distance measured from the wall toward its center, and b one half of the breadth of the channel. For studying in more detail the characteristics of flow behaviors, it becomes necessary to carry out the same calculation as was performed by HAYASHI. TABLE 1 embodies the results of the computation for the velocity profiles

$\alpha°$	δ_1/b	ϑ/b	H	γ
4	0.312	0.1755	1.777	0.474
3	0.246	0.1584	1.556	0.570
2	0.1994	0.1385	1.439	0.621
1	0.1541	0.1161	1.327	0.684
0	0.1008	0.0807	1.249	0.737
-2	0.0431	0.0365	1.181	0.764
-4	0.0213	0.01871	1.140	0.790
-8	0.01053	0.00957	1.101	0.843

TABLE 1.

obtained from the original figure by means of photographic enlargement. α denotes one half of the diverging ($\alpha > 0$) or the converging ($\alpha < 0$) angle of the channel;[1] γ will be referred to later (see equation (4.1)). Incidentally, numerical values in this table show slight differences from those due to HAYASHI (see the table on p. 7 of his paper), which presumably result from errors of numerical integrations.

For values of y/ϑ chosen at intervals of 0.1, u/u_0 is evaluated through the figure,[2] and employing these data, the velocity defect D_c (the subscript c refers to channels) for $\alpha = \alpha_*$, $y/\vartheta = y_*/\vartheta$ is defined in the same way as in (2.1):

$$D_c \equiv \frac{u}{u_0}\left(\alpha_*, \frac{y_*}{\vartheta}\right) - \frac{u}{u_0}\left(0, \frac{y_*}{\vartheta}\right). \tag{2.2}$$

Correspondence between the second terms on the right-hand sides of equations (2.1) and (2.2), or, in other words, between velocity distributions in the boundary layer along a flat plate and in the channel with parallel walls, might be justified by the well-known fact that the 1/7th power law of velocity profiles induced from measurements in the latter is found also to be valid approximately, within a certain range of REYNOLDS numbers, for boundary layers having no pressure gra-

1) NIKURADSE found that the first occurrence of separation of the forward flow at either wall happened between $\alpha = 4.8°$ and $5.1°$, cf. p. 22 of his paper, or GOLDSTEIN, S., *op. cit.*, **166**, p. 372.

2) Use is made of the relation $y/b = (y/\vartheta)\times(\vartheta/b)$. It should be noted, by the way, that in the original paper by NIKURADSE, y is taken in the reversed direction to this note (namely from the center toward the walls), and that the maximum speed denoted as u_0 here is written U there.

dient along streamlines.

In FIGURES 1 and 2, D_{tb} and D_c are shown for various values of y/ϑ, the abscissa. In the former, H is introduced as a parameter, and in the latter, α.

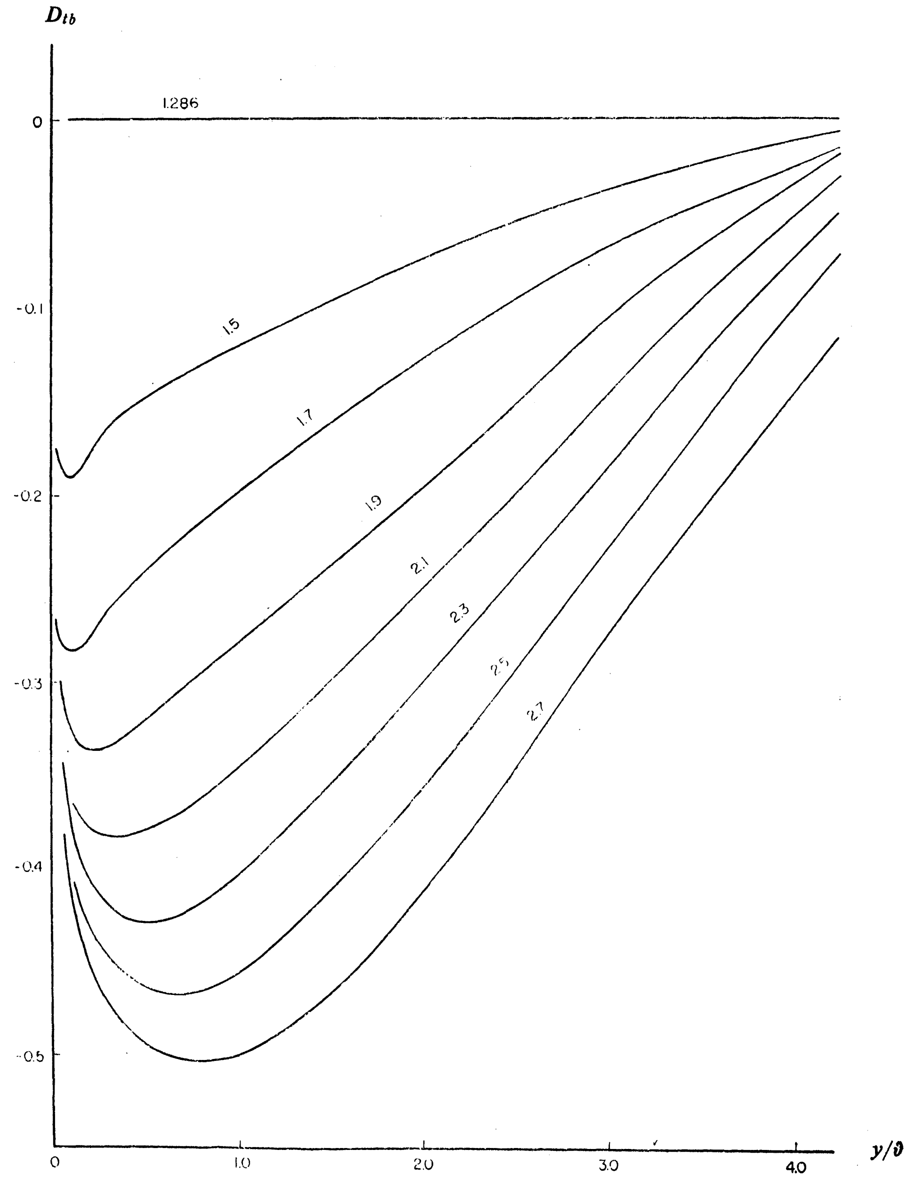

FIGURE 1. Velocity defects in turbulent boundary layers.
The number attached to each curve denotes the corresponding value of H.

Since velocity profiles in accelerating boundary layers which are to correspond to flows in converging channels are not included in *FIGURE 10* of VON DOENHOFF

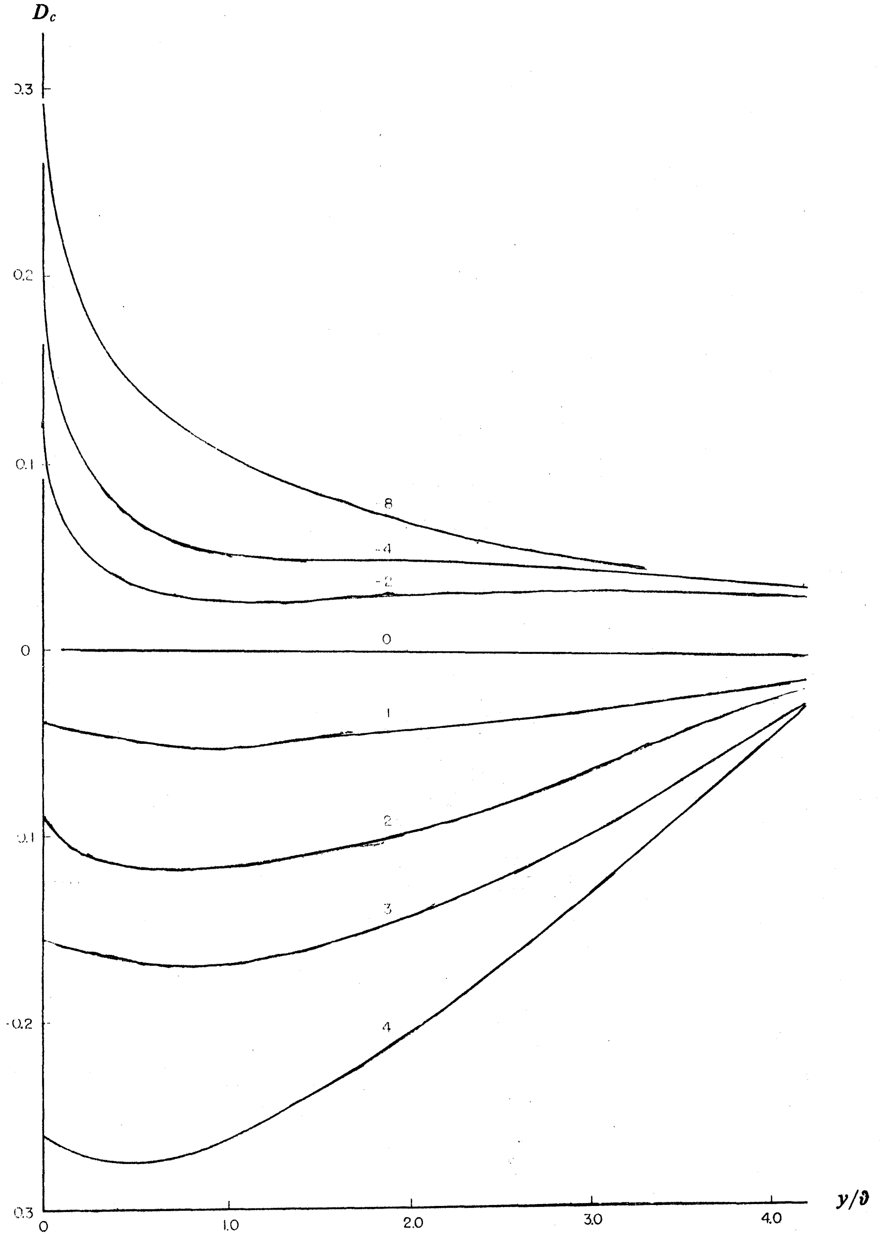

FIGURE 2. Velocity defects in channel flows.
The number attached to each curve denotes the corresponding value of α in degree.

and TETERVIN's paper, it is not possible to compare one with the other. However, contrast between the velocity defects of retarding boundary layers and of diverging channels might be clear. Namely, although each curve of D_{tb} has a deep and well-defined trough in the range $y/\vartheta < 1$, it is not distinct nor deep for a curve of D_c.

3. LUDWIEG-TILLMANN's law

Let us denote by u_ϑ the value of u at the point where y is equal to ϑ. If we assume that the form

$$u/u_\vartheta = (y/\vartheta)^n \tag{3.1}$$

could be valid generally, then by taking the logarithms of the both hand sides, we obtain

$$\log\frac{u}{U} = \log\frac{u_\vartheta}{U} + n\log\frac{y}{\vartheta}\ , \tag{3.2}$$

where as log and U we mean common logarithm and a typical velocity, respectively. By choosing u_1, the velocity of the main flow just outside the boundary layer, as U, LUDWIEG and TILLMANN plotted the correlation between $\log(u/u_1)$ and $\log(y/\vartheta)$ for velocity profiles measured in four cases of i) uniform pressure distribution along streamlines (zero pressure gradient), ii) moderate rise of pressure, iii) strong rise of pressure, and iv) fall of pressure (see footnote 5 on p. 73). By this means they arrived at the conclusion that quite an accurate linearity predicted by (3.2) does hold in the range of y less than ϑ. They also remarked that the family of these straight lines are all parallel (gradient n = constant) and that the value of n is approximately 0.13 irrespective of variations of REYNOLDS number and of pressure gradients in the direction of the stream (see p. 289 of the original papar).

Now, with a view to scrutinizing the accuracy of this law, curves of FIGURE 3 were constructed by reading the relation between $\log(u/u_1)$ and $\log(y/\vartheta)$ for the family of velocity profiles analyzed by VON DOENHOFF and TETERVIN (*FIGURE 10* of the original paper), while on the other hand FIGURE 4 was obtained through the same procedure for velocity distributions measured by NIKURADSE (*ABBILDUNG 10* of the original paper). In the latter case, however, u_0, the velocity of flow on the center line of the channel was taken as U.

The followings might be mentioned by examining both of our figures:

i) Despite of the conclusion by LUDWIEG and TILLMANN, results arrived at by plotting in great detail the velocity profiles in boundary layers and in channels reveal that the theory is valid, in reality, only approximately in both cases. Namely, for boundary layers linear relationship of equation (3.2) is not accurate except the case when $H = 1.286$, and besides lines are found straighter for the value of y such that $0.5 > \log(y/\vartheta) > 0$ (or $3 > y/\vartheta > 1$) than in the region $\log(y/\vartheta) < 0$ (or $y/\vartheta < 1$), contrary to the opinion of LUDWIEG and TILLMANN. On the other hand, linearity is *less* apparent on the whole in channel flows.

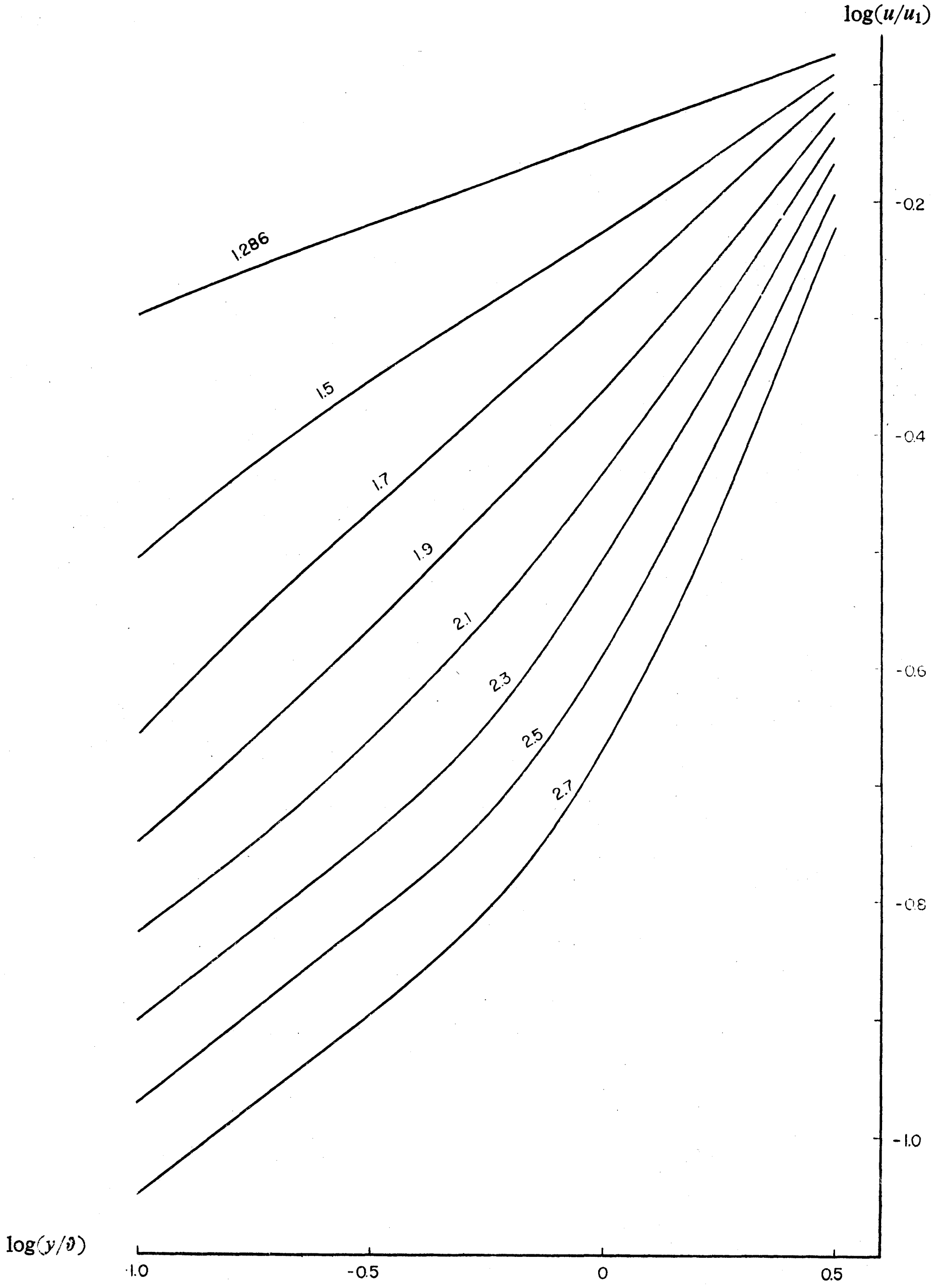

FIGURE 3. LUDWIEG-TILLMANN's law in boundary layers.
The number attached to each curve denotes the corresponding value of H.

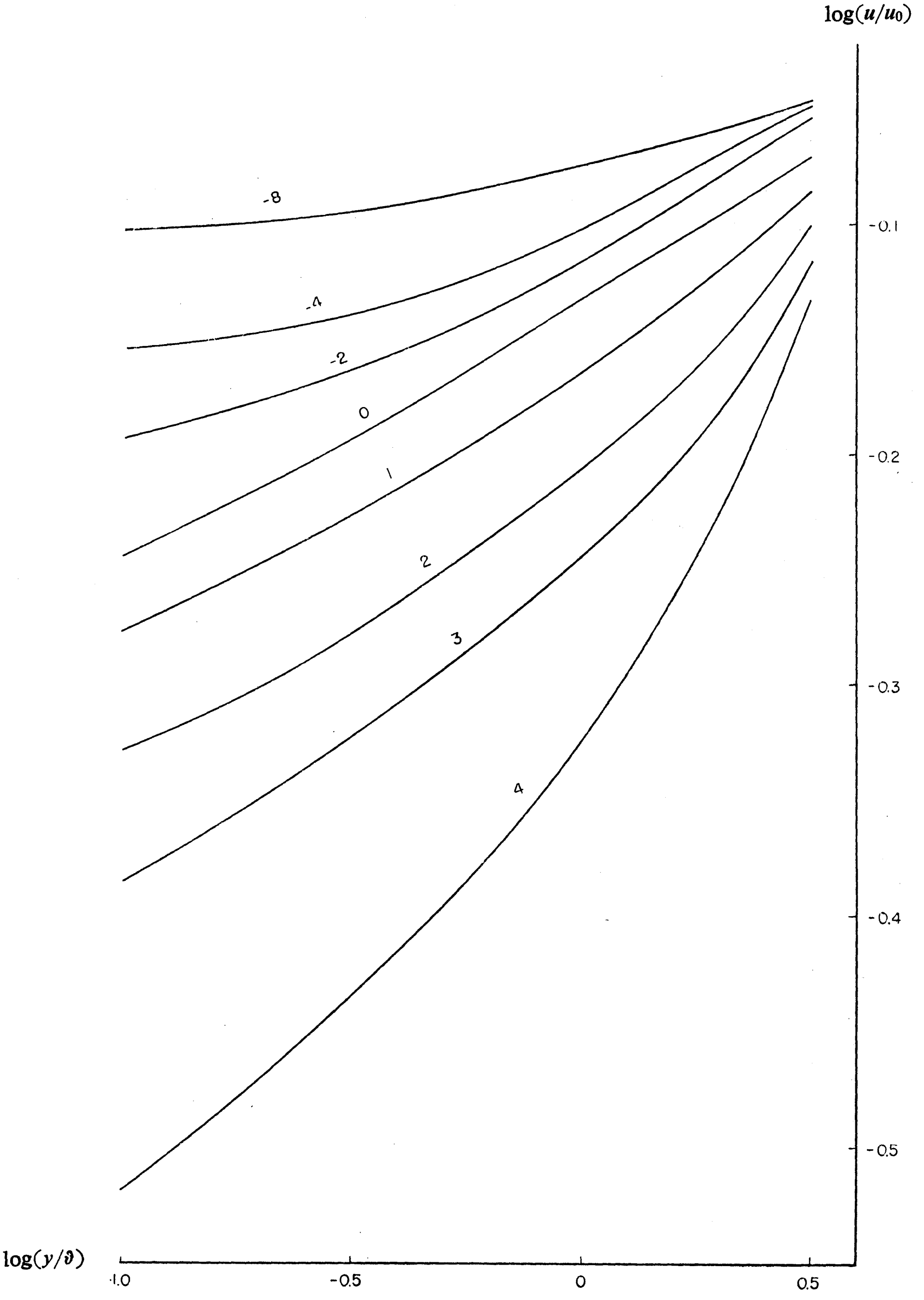

FIGURE 4. LUDWIEG-TILLMANN's law in channel flows.
The number attached to each curve denotes the corresponding value of α in degree.

ii) Again, despite of their second conclusion, the group of these curves are observed not parallel exactly to each other and their gradient (n) takes roughly the values which are shown by the followings :[1] TABLES 2 (boundary layer flows) and 3 (channel flows).

H	gradient n		
	0.5∼-0.5	0∼-1.0	mean value
1.286	0.15	0.15	0.15
1.5	0.26	0.28	0.27
1.7	0.36	0.37	0.37
1.9	0.44	0.39	0.41
2.1	0.52	0.42	0.47
2.3	0.58	0.38	0.48
2.5	0.62	0.39	0.50
2.7	0.67	0.38	0.53

TABLE 2.

$\alpha°$	gradient n		
	0.5∼-0.5	0∼-1.0	mean value
-8	0.05	0.03	0.04
-4	0.09	0.05	0.07
-2	0.11	0.08	0.09
0	0.12	0.11	0.12
1	0.14	0.11	0.13
2	0.18	0.12	0.15
3	0.21	0.14	0.17
4	0.30	0.20	0.25

TABLE 3.

iii) Furthermore, for the sake of comparison, similar results in laminar boundary layers (see FIGURE A-3 in appendix) is summarized in TABLE 4. The value of n is found much larger than in the preceding two kinds of flows.

Λ	gradient n	Λ	gradient n
3	0.90	-6	1.14
0	0.95	-9	1.33
-3	1.03	-12	1.79

TABLE 4.

4. PRETSCH'S formula

In terms of u_ϑ introduced in the preceding section, let us define in the first place the parameter

$$\gamma \equiv u_\vartheta / U, \tag{4.1}$$

where U denotes a typical velocity, representing for a boundary layer the velocity of the main flow just outside (u_1), and for a channel flow the velocity on its

1) The slopes of these curves were computed roughly by taking difference of the values of log (u/u_1) between two points appropriately chosen on the curve. In the above tables the first figure gives the difference between the points $\log(y/\vartheta) = 0.5$ and -0.5, and the second, between $\log(y/\vartheta) = 0$ and -1.0, the third being the average value of the first and the second. However, in TABLE 4 only the first figures (corresponding to 0.5∼-0.5) are shown.

center line (u_0), respectively. The parameter introduced by GRUSCHWITZ,

$$\eta \equiv 1-(u_\vartheta/u_1)^2 , \tag{4.2}$$

may be readily derived from γ according to the relationship

$$\eta = 1-\gamma^2 . \qquad (4.3)^{1)}$$

If we confine ourselves to flows in boundary layers for short, by assuming the velocity distribution in a power form

$$u/u_1 = (y/\delta)^n , \tag{4.4}$$

the followings may be obtained from the definitions of the displacement, and the momentum, thicknesses:

$$\delta_1/\delta = n/(n+1) , \tag{4.5}$$

$$\vartheta/\delta = n/(n+1)(2n+1) , \tag{4.6}$$

and

$$H = 2n+1, \quad \text{or} \quad n = (H-1)/2 . \tag{4.7}$$

Combining (4.1) with (4.4), we have therefore

$$\gamma \equiv \frac{u_\vartheta}{u_1} = \left(\frac{\vartheta}{\delta}\right)^n = \left\{\frac{H-1}{H(H+1)}\right\}^{(H-1)/2} , \tag{4.8}$$

and substituting (4.8) for (4.3), we may write also

$$\eta = 1- \left\{\frac{H-1}{H(H+1)}\right\}^{H-1} , \tag{4.9}$$

as the relation connecting η with H.[2] (4.8) or (4.9) is referred to as PRETSCH's formula. It is worthy of noting that, in spite of a very bold assumption of expressing the velocity profile in a power form of distance from the wall, equation (4.8) (or (4.9)) may be regarded as a very accurate representation for the correlation between H and γ (or η) induced out of miscellaneous experimental work. That is to say, GRANVILLE compared equation (4.8) with measurements by GRUSCHWITZ,[3] again SCHLICHTING, the same equation with experiments by NIKURADSE, GRUSCHWITZ, and KEHL.[4] By both of those comparisons good agreement was verified between the approximate expression (4.8) and observations of these authors. Incidentally the following empirical formula was proposed between γ and H by LUDWIEG and TILLMANN:

$$\gamma = 2.333\cdot 10^{-0.398H} . \qquad (4.10)^{5)}$$

In FIGURE 5, equations (4.8) and (4.10) are drawn in a full, and a broken, lines

1) GOLDSTEIN, S., *op. cit.*, **213**, eq. (1), p. 487.

2) SCHLICHTING, H., *Boundary Layer Theory* (translated by KESTIN, J.)(1960), XXII, **b**, eq. (22.5), p. 570.

3) GRANVILLE, P. S., *ibid.*, Fig. 4, p. 8.

4) SCHLICHTING, H., *op. cit.*, Fig. 22.6, p. 571.

5) LUDWIEG, H. und TILLMANN, W., *ibid.*, Abb. 5, S. 296, where, however, the notation H_{12} is used in place of H.

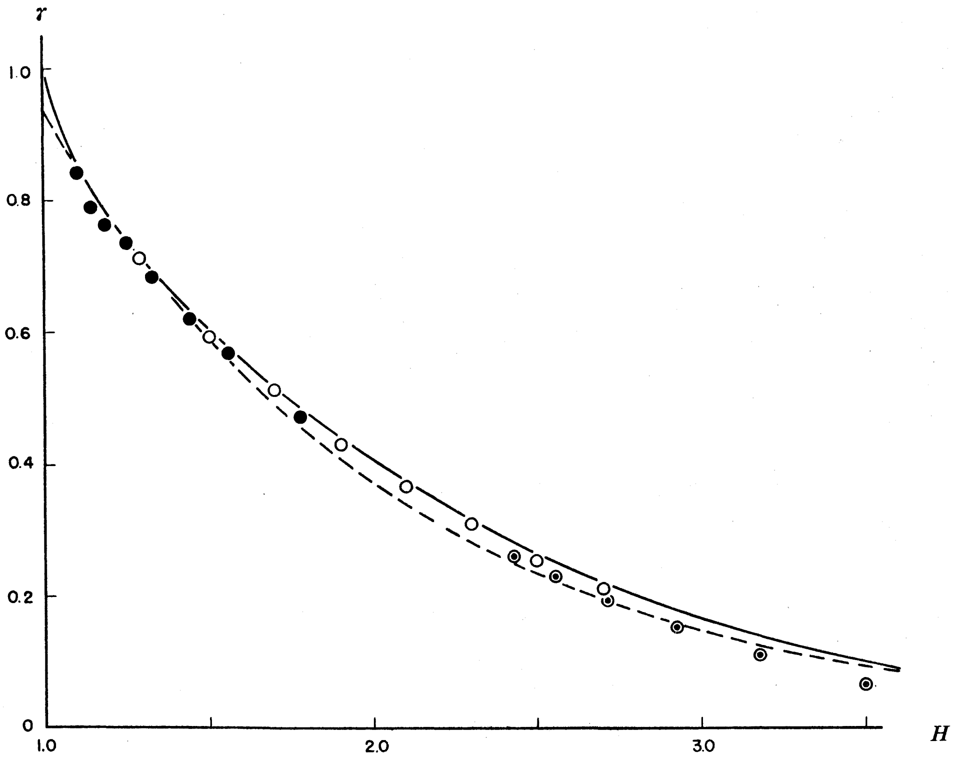

FIGURE 5. Relation between γ and H.

—— equation (4.8) ○ turbulent boundary layers
● turbulent channel flows
- - - equation (4.10) ⊙ laminar boundary layers

H	γ
1.286	0.714
1.5	0.594
1.7	0.515
1.9	0.433
2.1	0.369
2.3	0.311
2.5	0.256
2.7	0.214

TABLE 5.

Λ	δ_1/δ	ϑ/δ	H	γ
3	0.275	0.113	2.427	0.263
0	0.300	0.117	2.554	0.232
-3	0.325	0.120	2.716	0.195
-6	0.350	0.120	2.921	0.155
-9	0.375	0.118	3.176	0.112
-12	0.400	0.114	3.500	0.067

TABLE 6.

respectively, besides is plotted the relation between γ and H, derived from velocity profiles measured in turbulent boundary layers (symbol ○, VON DOENHOFF and

TETERVIN, *op. cit.*, *FIGURE 10*, see TABLE 5), from those in channels (symbol ●, NIKURADSE, *op. cit.*, *ABBILDUNG 10*, see TABLE 1), and also from those in laminar boundary layers (symbol ⊙, polynomial approximation according to POHLHAUSEN, cf. appendix, see TABLE 6). In all cases including that of laminar flow, it will be remarked that the relation expressed by (4.8) agrees quite satisfactorily with the former two empirical results and the remaining one theory. In other word, despite of the fact that equations (4.8) and (4.9) were both derived by assuming in particular a power law for velocity profiles, we might suppose that these results in themselves stand (at least, approximately) for a property of much more general character. As mentioned in section 1, contents of this section are well-known facts, only added with a view to re-affirming the general validity of (4.8) with the aid of new data of measurements for boundary layers and flows in channels.

5. Distribution of shearing stress

As to the distribution of shearing stress τ in boundary layers, FEDIAEVSKY proposed a computation in which τ is assumed in the form of a polynomial with regard to y, normal distance from the wall, and the coefficient of each term is to be determined in such a way that the conditions imposed upon the shearing stress would be satisfied on the surface of the wall ($y=0$) as well as on the outer edge of the boundary layer ($y=\delta$) (see footnote 2 on p. 74). Namely, denoting by τ_0 the value of τ on the wall, let us put

$$\frac{\tau}{\tau_0} = A_0 + A_1\left(\frac{y}{\delta}\right) + A_2\left(\frac{y}{\delta}\right)^2 + \cdots + A_n\left(\frac{y}{\delta}\right)^n, \tag{5.1}$$

where in general the coefficients A's are functions of x, the coordinate measured along the surface of a body.

On the other hand, since the equation of mean motion in the boundary layer may be written approximately

$$u\frac{\partial u}{\partial x} + v\frac{\partial u}{\partial y} = -\frac{1}{\rho}\frac{\mathrm{d}p}{\mathrm{d}x} + \frac{1}{\rho}\frac{\partial \tau}{\partial y}, \tag{5.2}$$

where u and v are the x-, and the y-, components respectively of the mean velocity, ρ and p being the density, and the mean pressure, of the fluid. $A_0, A_1, \ldots, A_n$ can be determined with the aid of the following conditions:

i) At $y=0$, from the definition of τ_0,

$$\tau/\tau_0 = 1\,. \tag{5.3}$$

ii) At $y=0$, since the left-hand side of equation (5.2) vanishes, we have accordingly

$$\partial\left(\frac{\tau}{\tau_0}\right)\Big/\partial\left(\frac{y}{\delta}\right) = \frac{\delta}{\tau_0}\frac{\mathrm{d}p}{\mathrm{d}x}\,. \tag{5.4}$$

iii) Differentiating (5.2) with respect to y, and substituting the equation of continuity of the mean motion, we have at $y=0$

$$\partial^2\left(\frac{\tau}{\tau_0}\right)\Big/\partial\left(\frac{y}{\delta}\right)^2 = 0\,. \tag{5.5}$$

iv) Owing to the condition of smooth vanishing of τ on the outer edge of the boundary layer, at $y = \delta$ it must be that

$$\tau/\tau_0 = 0, \tag{5.6}$$

and that

v)
$$\partial\left(\frac{\tau}{\tau_0}\right)\Big/\partial\left(\frac{y}{\delta}\right) = 0. \tag{5.7}$$

Now if we assume a polynomial of degree four with respect to y/δ and determine five coefficients from these five conditions, then we should readily obtain

$$\begin{gathered} A_0 = 1, \quad A_1 = \frac{\delta}{\tau_0}\frac{\mathrm{d}p}{\mathrm{d}x}, \quad A_2 = 0, \\ A_3 = -4-3\frac{\delta}{\tau_0}\frac{\mathrm{d}p}{\mathrm{d}x}, \quad \text{and} \quad A_4 = 3+2\frac{\delta}{\tau_0}\frac{\mathrm{d}p}{\mathrm{d}x}. \end{gathered} \tag{5.8}$$

On the other hand, however, by taking a polynomial of degree three and employing only four conditions i), ii), iv), and v) (two conditions on the wall, and two on the outer edge of the boundary layer), we are led to the result

$$\begin{gathered} A_0' = 1, \ A_1' = \frac{\delta}{\tau_0}\frac{\mathrm{d}p}{\mathrm{d}x}, \ A_2' = -3-2\frac{\delta}{\tau_0}\frac{\mathrm{d}p}{\mathrm{d}x}, \\ \text{and} \qquad A_3' = 2+\frac{\delta}{\tau_0}\frac{\mathrm{d}p}{\mathrm{d}x}. \end{gathered} \tag{5.9}$$ [1]

Again, if we choose another combination of four conditions i), ii), iii), and iv) in order to set more importance on flow behaviors in the immediate neighborhood of the solid surface, then we should arrive at

$$\begin{gathered} A_0'' = 1, \quad A_1'' = \frac{\delta}{\tau_0}\frac{\mathrm{d}p}{\mathrm{d}x}, \quad A_2'' = 0, \\ \text{and} \qquad A_3'' = -1-\frac{\delta}{\tau_0}\frac{\mathrm{d}p}{\mathrm{d}x}. \end{gathered} \tag{5.10}$$

Later SCHUBAUER and KLEBANOFF measured the distribution of shearing stress in the boundary layer and compared results with the representation (5.8). They state, 'The agreement between Fediaevsky's theory and experimental values from the present investigation was fair at the 17½-foot position and excellent at the 25-foot position, but elsewhere was poor' (see p. 8, esp. *FIGURE 16*, of the original paper cited in footnote 3 on p. 74). In their experiment, the 17½-, and the 25-, foot positions of the airfoil placed in the wind tunnel are the point of the minimum pressure and the neighborhood of separation, respectively. Furthermore, in the region of pressure rise, taking also into account of hysteresis effects in boundary layers, Ross and ROBERTSON adopted the condition

v)′ at $y = \delta$

---

1) This simplification was introduced by FEDIAEVSKY himself. However, on p. 493 of his paper, *for* '(b) For conditions I, II, III, and IV' *read* '…I, II, III, and V'.

$$\partial\left(\frac{\tau}{\tau_0}\right)\Big/\partial\left(\frac{y}{\delta}\right) = -\frac{\tau_{0m}\,\delta}{\tau_0\,\delta_m} \tag{5.11}$$

in place of v), where τ_{0m} and δ_m denote the values of τ_0 and δ respectively at the starting point of the region, the point of the minimum pressure in other words.[1] Comparing their results with the experimental data (shear profiles obtained at the National Bureau of Standards for boundary layer flow in an adverse pressure gradient[2]), they conclude that owing to this improvement the mathematical expression for shearing stress is able to reproduce the actual situation almost completely for locations near the beginning of the adverse pressure gradient (the 20-foot station) and near separation (the 25-foot station) and fairly well for location midway toward separation (the 22.5-foot station) (see *FIGURES 3* and *4* of ROSS and ROBERTSON's paper). By the way, according to them, FEDIAEVSKY's original formula brings about only poor agreement with measurements at the location of the minimum pressure, the fact inconsistent with the remarks by SCHUBAUER and KLEBANOFF.

We now ask the question: 'How successfully may be applied the similar method to flows in channels?' Confining ourselves to the original theory of FEDIAEVSKY, without employing the improvement due to ROSS and ROBERTSON, we put $y = b$ in place of $y = \delta$ for conditions iv) and v). However, in order to determine the coefficients of a polynomial by the aid of (5.8), (5.9), or (5.10), it is necessary to evaluate a parameter defined by $b\mathrm{d}p/\tau_0\mathrm{d}x$, namely $b\times(\mathrm{d}p/\rho\mathrm{d}x)\div(\tau_0/\rho)$.

i) Values of b (one half of the breadth of the channel, cm) are listed in *ZAHLENTAFEL 1* of NIKURADSE's paper (S. 11, Meßquerschnitt III) as follows:

$$\begin{gathered}2.70\ (\alpha = 4^\circ),\ 2.15\ (3^\circ),\ 1.65\ (2^\circ),\ 1.10(1^\circ),\\ 0.60(0^\circ),^{3)}\ 1.02(-2^\circ),\ 1.44(-4^\circ),\ 2.28(-8^\circ).\end{gathered} \tag{5.12}$$

ii) $\mathrm{d}p/\rho\mathrm{d}x$ (pressure gradient, cm/sec²) is given in *ZAHLENTAFEL 13* (S. 45) of the paper, namely

$$\begin{gathered}510(\alpha = 4^\circ),\ 804(3^\circ),\ 1085(2^\circ),\ 1725(1^\circ),\\ -1630(0^\circ),\ -5460(-2^\circ),\ -3730(-4^\circ),\ -1830(-8^\circ).\end{gathered} \tag{5.13}$$

iii) Also τ_0/ρ(shearing stress on the wall, cm/sec²) is shown in the same table:[4]

$$30(\alpha = 4^\circ),\ 75(3^\circ),\ 150(2^\circ),\ 310(1^\circ),$$

---

1) ROSS, D. and ROBERTSON, J. M., Shear Stress in a Turbulent Boundary Layer, *Journal of Applied Physics*, vol. 21 (1950), no. 6, pp. 557-561.

2) DRYDEN, H. L., Some Recent Contributions to the Study of Transition and Turbulent Boundary Layers, *NACA Technical Note*, no. 1168 (1947), esp. Figs. 10 and 11.

3) 0.00 in the original table is supposed to be misprinted.

4) *ZAHLENTAFEL 8* (S. 32), in which τ/ρ is listed for various values of y, gives for $y = 0$ values slightly different from those mentioned above. Namely, they are 30 ($\alpha =$ 4°), 75(3°), 150(2°), 310(1°), 970(0°), 374(−2°), 200(−4°), and 95(−8°). *ZAHLENTAFEL 13* is supposed to be constructed by smoothing out the curves produced from *ZAHLENTAFEL 8*.

$$971(0^\circ),\ 375(-2^\circ),\ 220(-4^\circ),\ 95(-8^\circ). \tag{5.14}$$

Making use of these data, the coefficients $A_0, \ldots, A_4$ and $A_0'', \ldots, A_3''$ can be computed from conditions (5.8) and (5.10) as shown in TABLE 7 below:[1]

α°	A_1	A_3	A_4	A_1''	A_3''	B_1	B_3	B_4
4	45.90	-141.70	94.80	45.90	-46.90			
3	23.05	-73.14	49.10	23.05	-24.05			
2	11.94	-39.81	26.87	11.94	-12.94			
1	6.121	-22.363	15.242	6.121	-7.121			
0	-1.0072	-0.9784	0.9856	-1.0072	0.0072			
-2	-14.85	40.55	-26.70	-14.85	13.85	-12.25	32.76	-21.50
-4	-24.41	69.24	-45.83	-24.41	23.41	-14.65	39.95	-26.30
-8	-43.92	127.76	-84.84	-43.92	42.92	-17.02	47.06	-31.04

TABLE 7.

Substituting these values for the coefficients, τ/τ_0 may be worked out for various values of y/b in the form

$$\frac{\tau}{\tau_0} = A_0 + A_1\left(\frac{y}{b}\right) + A_3\left(\frac{y}{b}\right)^3 + A_4\left(\frac{y}{b}\right)^4, \tag{5.15}$$

or

$$\frac{\tau}{\tau_0} = A_0'' + A_1''\left(\frac{y}{b}\right) + A_3''\left(\frac{y}{b}\right)^3; \tag{5.16}$$

the result of these calculations is reproduced in FIGURES 6-1 through 6-8; full lines and broken lines correspond to (5.15) and (5.16) respectively.

On the other hand, *ZAHLENTAFEL 10* (S. 37) gives the distribution of shearing stress obtained in experimental works by NIKURADSE, which is reprinted in terms of our notations as TABLES 8-1 through 8-8 at the end of this paper, y' being distance (cm) measured from the center of the channel toward the wall. Namely there exists the relation

$$y + y' = b \tag{5.17}$$

between y and y'. Values of τ/ρ for $y' = b$ (or $y = 0$) were shown already as τ_0/ρ. In FIGURES 6 experimental values of τ/τ_0 are indicated by white circles.

Comparing the computed values of τ/τ_0 with those obtained by measurements in channels, we may derive some conclusions with regard to the validity of polynomial representation for the distribution of shearing stress in channel flows, which might be summarized as follows:

i) Corresponding to SCHUBAUER and KLEBANOFF's remarks that in turbulent

1) Of the polynomials of degree four with coefficients (5.9) and (5.10), only the one associated with A'''s is tested in order to avoid unnecessary duplications. As to B_1, B_3, and B_4 in the same table, see footnote 1, p. 89, esp. eq. (F.1).

boundary layers FEDIAEVSKY's theory for the distribution of shearing stress yields results quite satisfactory at location near the positions of the minimum pressure and near separation but that the coincidence is found very poor for points midway toward separation, similar technique applied to channel flows results in agreement fairly good for both $\alpha = 0°$ (parallel walls) and $\alpha = 4°$ (roughly the limit up to which symmetry of flow is maintained), but approximation is found quite poor for angles intermediate between them, α being one half of the diverging ($\alpha > 0$) or of the converging ($\alpha < 0$) angle of a channel.

ii) Except the case $\alpha = 0°$, better agreement with measurements is attained by equations (5.8)-(5.15), the polynomial of degree four determined by means of five boundary conditions, than by equations (5.10)-(5.16), that of degree three constructed with the aid of four conditions.

iii) For a negative α (a converging channel), polynomial method fails completely to approximate the real distribution.[1] In this case, however, as to comparison with boundary layer no definite conclusion can be drawn, since nothing was mentioned by SCHUBAUER and KLEBANOFF (*ibid.*) nor by DRYDEN (*ibid.*) concerning boundary layers in the region of pressure drop.

---

1) As an improvement of approximation for converging channels, the following computations were performed tentatively. In view of the fact that velocity profiles measured by NIKURADSE are very flat for converging channels, let us suppose the 'boundary layer thickness' δ, so to speak, along the walls of a channel and outside it the flow is assumed free from all influences of walls. In (5.8), the new A_1 (let us write B_1), for instance, should be $\delta dp/\tau_0 dx$ instead of $b dp/\tau_0 dx$ and so equal to $(\delta/b) \times (b dp/\tau_0 dx)$, which may be evaluated from the former A_1. In a similar manner, all the modified coefficients can be obtained without difficulty (also see TABLE 7):

$$B_0 = 1,\quad B_1 = \left(\frac{\delta}{b}\right)\left(\frac{b}{\tau_0}\frac{dp}{dx}\right),\quad B_2 = 0,$$
$$B_3 = -4-3\left(\frac{\delta}{b}\right)\left(\frac{b}{\tau_0}\frac{dp}{dx}\right), \tag{F.1}$$
and
$$B_4 = 3+2\left(\frac{\delta}{b}\right)\left(\frac{b}{\tau_0}\frac{dp}{dx}\right).$$

Thus the shearing stress may be expressed in the form

$$\frac{\tau}{\tau_0} = B_0+B_1\left(\frac{b}{\delta}\right)\left(\frac{y}{b}\right)+B_3\left(\frac{b}{\delta}\right)^3\left(\frac{y}{b}\right)^3 + B_4\left(\frac{b}{\delta}\right)^4\left(\frac{y}{b}\right)^4. \tag{F.2}$$

Now, out of the above-mentioned figure due to NIKURADSE, we may estimate δ/b for various values of α as follows.

$$\delta/b = 0.83\ (\alpha = -2°),\ 0.60\ (\alpha = -4°),$$
and
$$0.39\ (\alpha = -8°). \tag{F.3}$$

In FIGS. 6-6,-7,-8, the dotted curves show the distribution of τ given by (F.2). After all, however, no sensible improvement can be attained, thus the failure of approximation of FEDIAEVSKY's method when applied to converging channels should be attributed to the theory itself and not to the way of correspondence between the boundary layer thickness and the breadth of the channel.

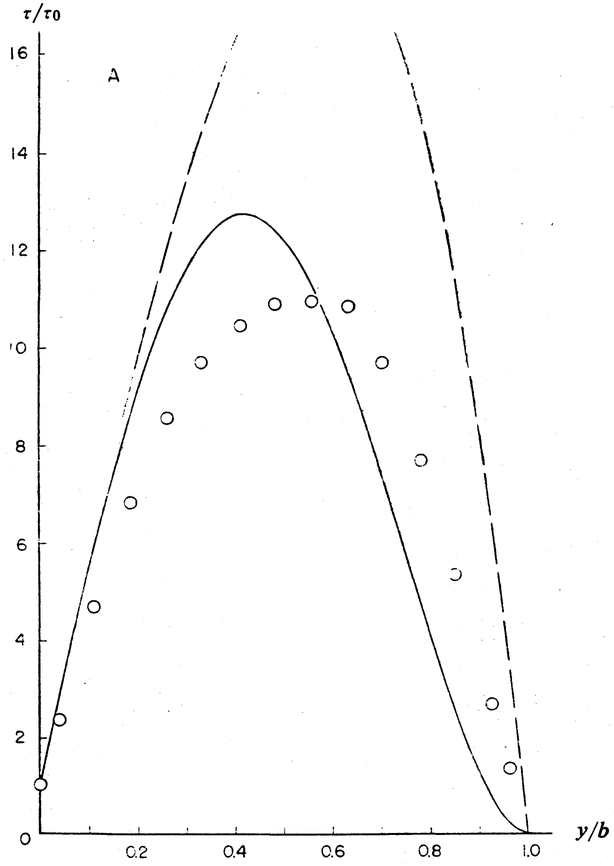

FIGURE 6-1. Distribution of shearing stress in channel flow ($\alpha=4°$).

—— equation (5.15)
– – – equation (5.16)
○ experiment by NIKURADSE

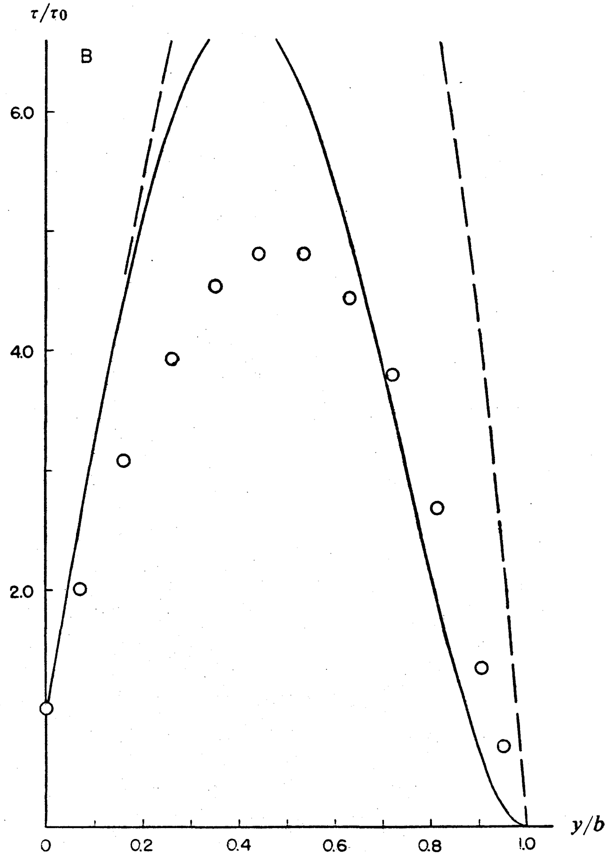

FIGURE 6-2. Distribution of shearing stress in channel flow ($\alpha=3°$).

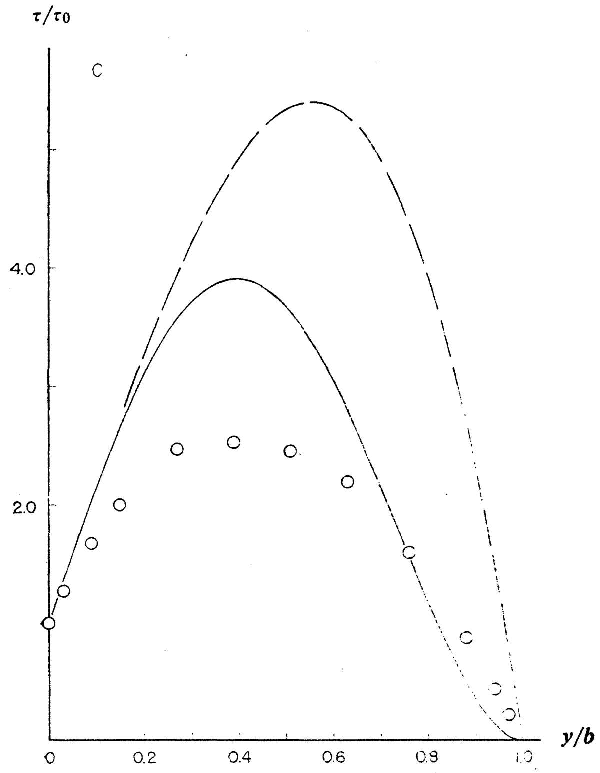

FIGURE 6-3. Distribution of shearing stress in channel flow ($\alpha=2°$).

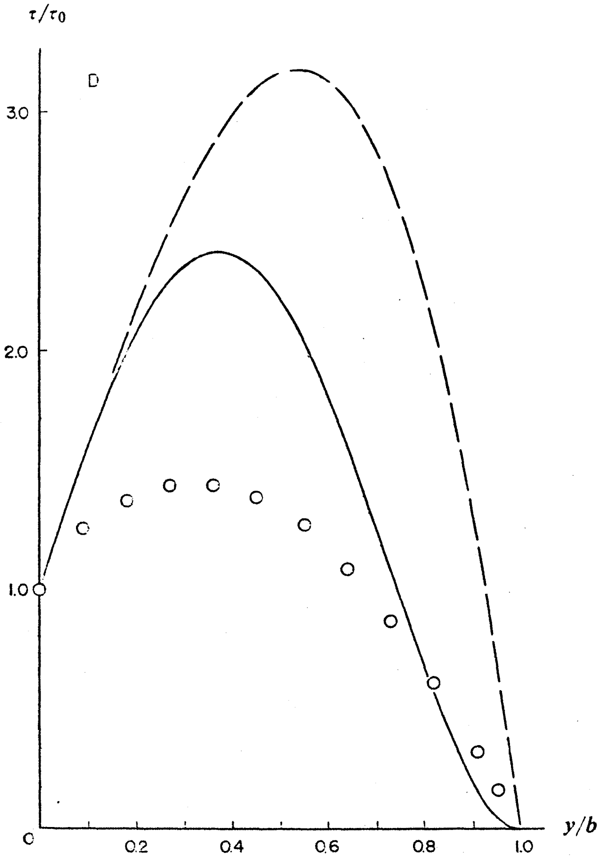

FIGURE 6-4. Distribution of shearing stress in channel flow ($\alpha=1°$).

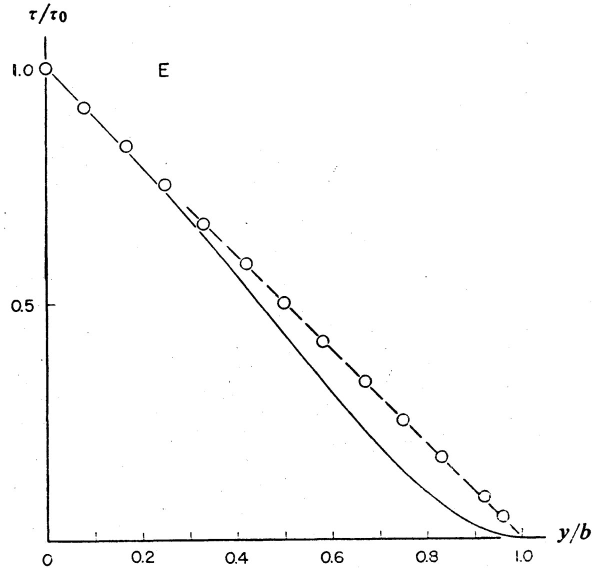

Figure 6-5. Distribution of shearing stress in channel flow ($\alpha = 0°$).

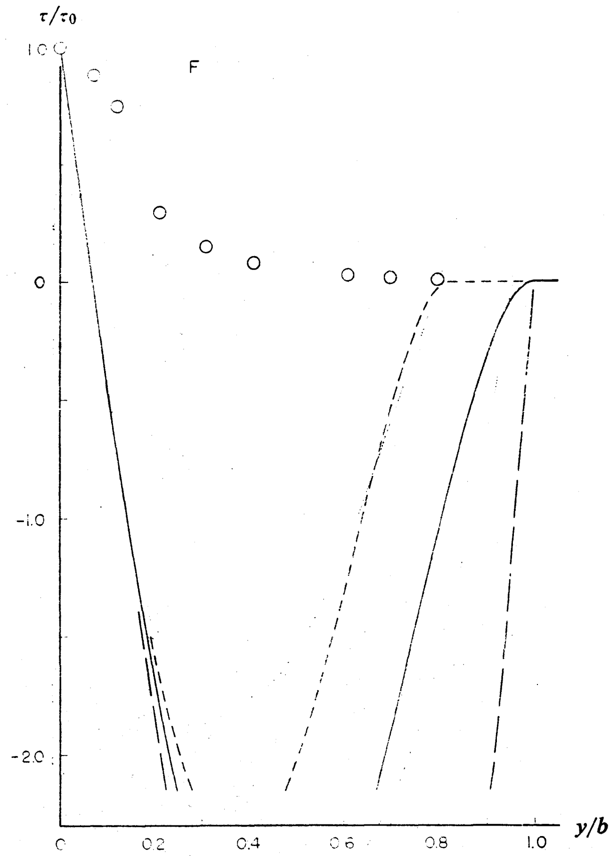

Figure 6-6. Distribution of shearing stress in channel flow ($\alpha = -2°$).

- - - - equation (F.2)

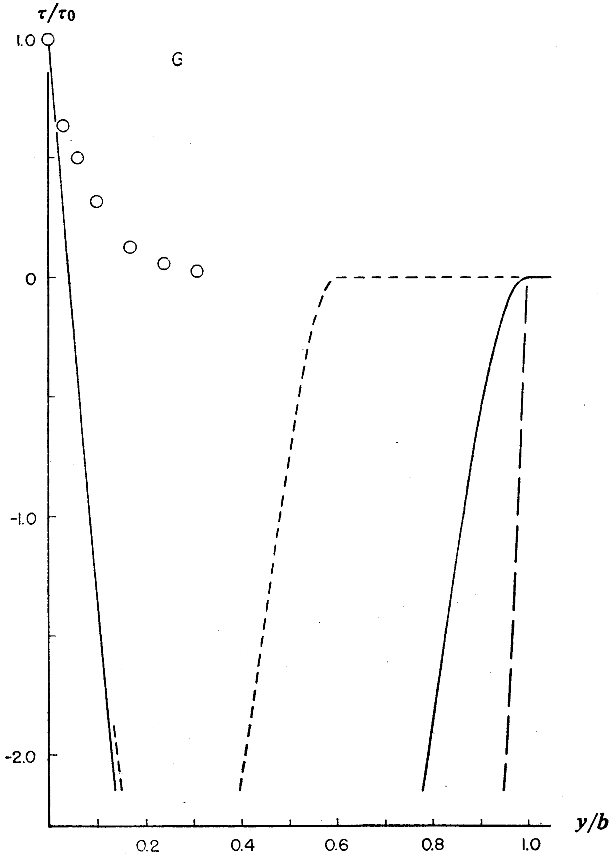

FIGURE 6-7. Distribution of shearing stress in channel flow ($\alpha = -4°$).

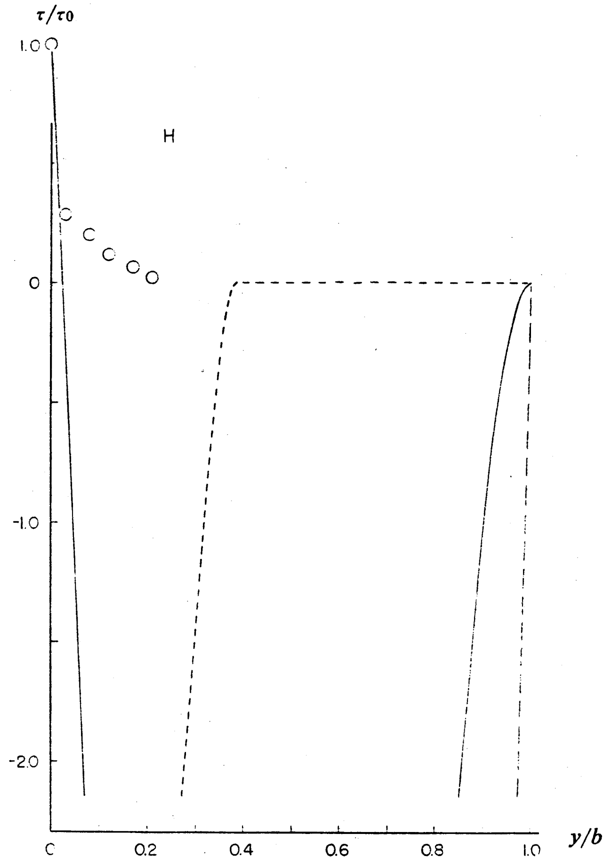

FIGURE 6-8. Distribution of shearing stress in channel flow ($\alpha = -8°$).

6. Functional forms of $H(\Gamma)$ and $\zeta(\Gamma)$

As a method of calculating turbulent boundary layers approximately, HOWARTH constructed a differential equation of the first order

$$\frac{d\chi}{dx'} + \frac{5}{4}\frac{\chi}{u_1'}\frac{du_1'}{dx'}(2+H) = \frac{5}{4}\frac{\zeta}{u_1'^{1/4}}, \tag{6.1}$$

where χ, u_1', x', ζ, and R_L are all non-dimensional quantities defined by

$$\begin{aligned} \chi &\equiv R_L^{1/4}\vartheta'^{5/4}, \\ u_1' &\equiv u_1/U, \quad x' \equiv x/L, \quad \vartheta' \equiv \vartheta/L, \\ \zeta &\equiv R_\vartheta^{1/4}(\tau_0/\rho u_1^2); \end{aligned} \tag{6.2}$$

and

$$R_L \equiv UL/\nu, \qquad R_\vartheta \equiv u_1\vartheta/\nu,$$

U and L being typical velocity and length respectively (see footnote 5 on p. 74). Further it was assumed that both of H and ζ were the known functions of the third quantity

$$\Gamma \equiv R_\vartheta^{1/4}\frac{\vartheta}{u_1}\frac{du_1}{dx} = R_L^{1/4}u_1'^{-3/4}\vartheta'^{5/4}\frac{du_1'}{dx'}, \tag{6.3}$$

their functional forms being given graphically in *FIGURES 10* and *11* (HOWARTH's paper) or *FIGURES 117* and *118* (GOLDSTEIN, *op. cit.*, p. 375). Data underlying these curves were taken for the most part from NIKURADSE's experiments (see footnote 2 on p. 73), and were supplemented with those due to BURI (see footnote 4 on p. 74). It should be remarked at this point, however, that both of these measurements were performed in channels,[1] and so some critical studies would be necessary before we may safely apply these functions to a boundary layer formed along a surface of a body.

For this purpose we shall perform two kinds of computations. In the first place, let us mention a calculation by VON DOENHOFF and TETERVIN applicable to turbulent boundary layers (see footnote 4 on p. 72). This treatment is reduced eventually to solving the three simultaneous differential equations of the first order with respect to the momentum thickness ϑ, the form parameter H, and the surface traction τ_0. ϑ/c and H computed as functions of x/c for the airfoil section NACA 65 (216)-222 (approx.) are shown in *FIGURES 22* (R_c, the REYNOLDS number referred to c, the chord of the airfoil, being 0.92×10^6; α, the angle of attack, 8.1°), *23*($R_c = 2.67\times10^6$; $\alpha = 8.1°$), and *24*($R_c = 2.64\times10^6$; $\alpha = 10.1°$) of the original paper (pp. 22-23), and agreement fairly good is attained for each of these examples in the whole range of x under examination. In *TABLE I* of their paper (p. 25), for the case $R_c = 2.64\times10^6$ and $\alpha = 10.1°$, various kinds of calculated quantities (namely, ϑ/c, H, q/q_0, $c\,dq/q_0dx$, R_ϑ, $\tau_0/\rho u_1^2$, and so on) are listed against the non-dimensional coordinate x/c, where q and q_0 stand for the dynamic pressure just outside the boundary layer and its initial value respectively, R_ϑ being

---

1) 'The measurements of Nikuradse were obtained from experiments in converging and diverging channels whilst those of Buri seem to be confined to converging channels.' ——HOWARTH, L., *ibid.*, 9, p. 576.

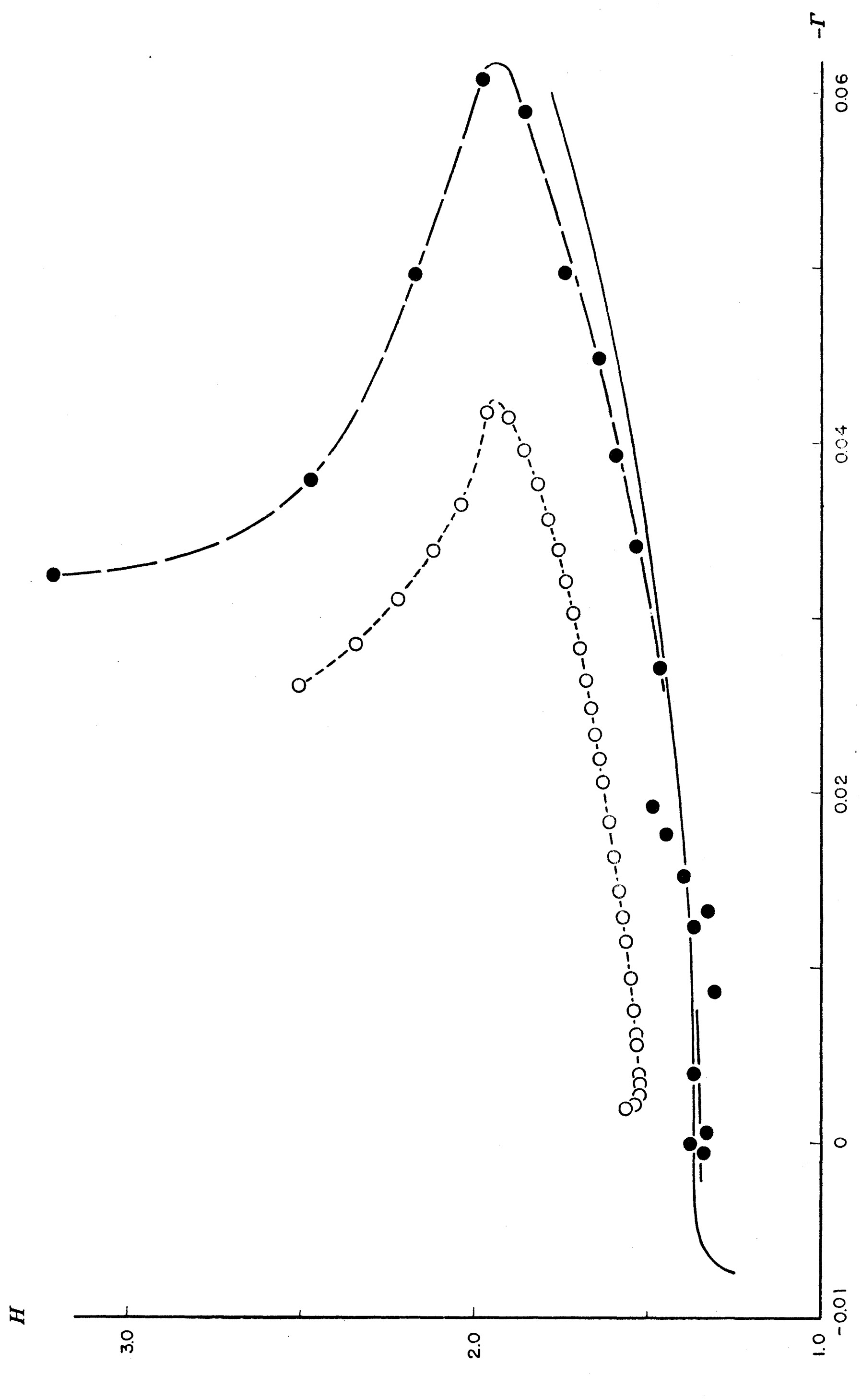

FIGURE 7. Relation between H and Γ.

—— HOWARTH

○ VON DOENHOFF and TETERVIN

● SCHUBAUER and KLEBANOFF

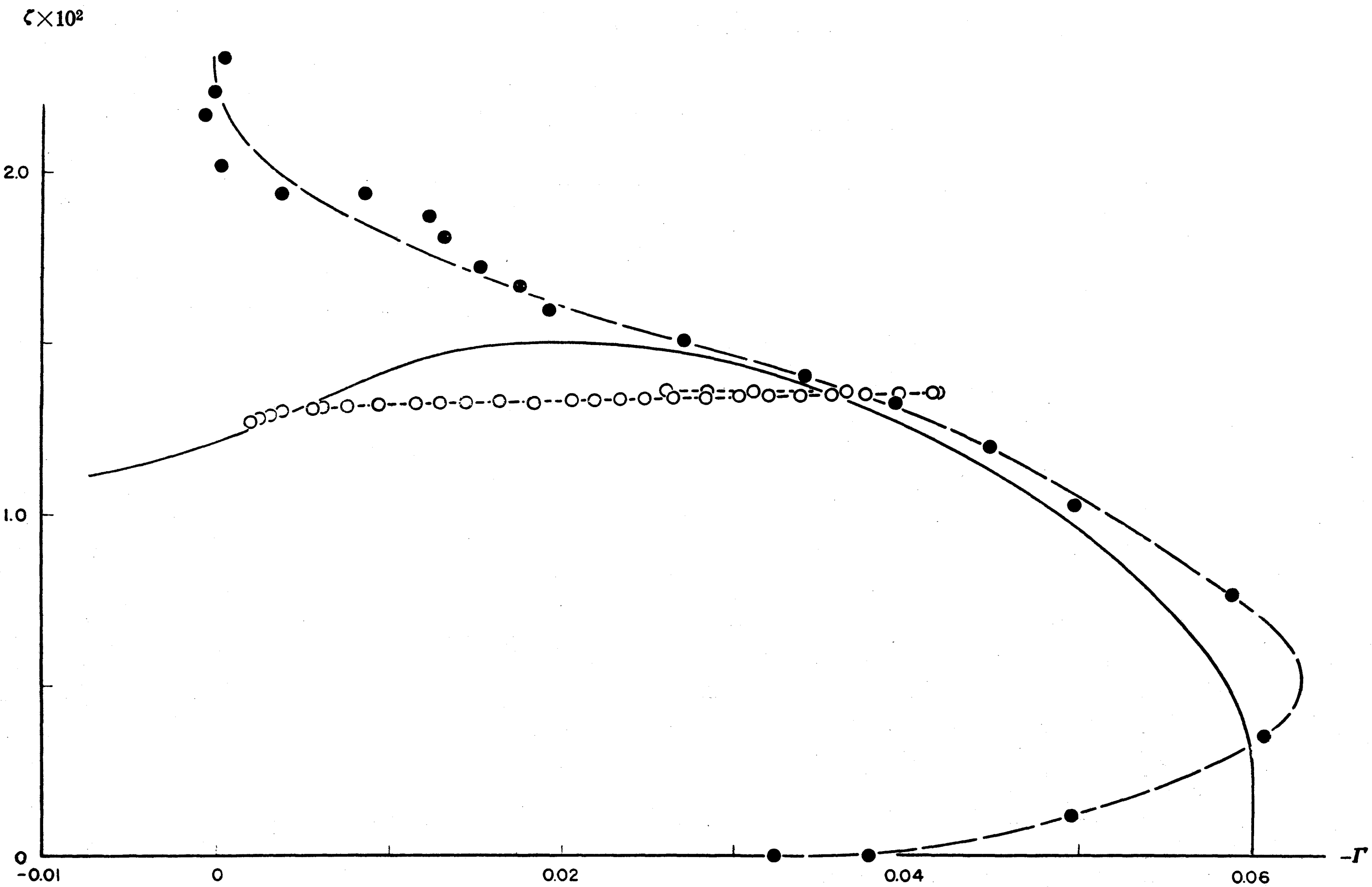

FIGURE 8. Relation between ζ and Γ.

—— HOWARTH
○ VON DOENHOFF and TETERVIN
● SCHUBAUER and KLEBANOFF

$u_1\vartheta/\nu$. It is not difficult to work out from these data the quantities necessary for us. H has been given already; ζ and Γ defined by (6.2) and (6.3) may be derived in the following way:

$$\zeta = R_\vartheta^{1/4}\tau_0/\rho u_1^2, \tag{6.4}$$

and

$$\Gamma = R_\vartheta^{1/4}\frac{\vartheta}{u_1}\frac{du_1}{dx}$$

$$= R_\vartheta^{1/4}\left(\frac{\vartheta}{c}\right)\left(\frac{1}{2}\frac{c}{q_0}\frac{dq}{dx} \div \frac{q}{q_0}\right). \tag{6.5}$$

Plots of H and ζ against Γ, all of which were computed out of VON DOENHOFF-TETERVIN's table, are marked by $\circ$ in FIGURES 7 and 8; in these figures the full lines are the reproductions of the curves due to HOWARTH.

Since, however, the preceding test is based upon a theoretical (or more precisely, semi-empirical) computation, it would be more desirable to compare HOWARTH's curves directly with experimental results obtained in boundary layers. One of them may be found in the paper by SCHUBAUER and KLEBANOFF (see footnote 3 on p. 74). So we shall take it up in the next place. Their investigation consists of measurements (by means of hot-wire technique) of various quantities characteristic of the boundary layer formed on an airfoil placed in a wind tunnel. Data available to us will be found in *TABLE 1* (distribution of dynamic pressure, p. 12 of their paper) and *TABLE 3* (boundary-layer parameters, p. 13) together with *FIGURE 17* (experimental values for coefficient of skin friction, p. 8). The first table gives the values of q_1/q_m for various values of x (ft), where q_1 and q_m are the free-stream dynamic pressure ($\frac{1}{2}\rho u_1^2$) and the free-stream dynamic pressure at $x=17\frac{1}{2}$ feet ($\frac{1}{2}\rho u_m^2$) respectively, u_m being the mean velocity just outside the boundary layer at the point $x = 17\frac{1}{2}$ feet (160 ft/sec) used as the reference velocity throughout their paper; q_1 and q_m correspond respectively to q and q_0 in VON DOENHOFF-TETERVIN's paper. The second table, on the other hand, shows values of δ_1 (δ^* in original notation, inch), ϑ (inch), and H for values of x (ft) collectively. Finally *FIGURE 17* gives the value of $C_f \equiv \tau_0/\frac{1}{2}\rho u_1^2$ vs. x. Through similar transformations as before we are enabled to deduce necessary quantities out of them:

$$R_\vartheta \equiv \frac{u_1\vartheta}{\nu} = \frac{u_m L}{\nu}\left(\frac{q_1}{q_m}\right)^{1/2}\frac{\vartheta}{L}$$

$$= 14{,}300{,}000\left(\frac{q_1}{q_m}\right)^{1/2}\frac{\vartheta}{L}, \tag{6.6}$$ [1)]

$$(L = 14.3 \text{ ft})$$

in terms of which we may write from (6.4) and (6.5) above

$$\zeta = R_\vartheta^{1/4}\frac{C_f}{2},$$

1) 'The speed (u_m) was always adjusted for changes in kinematic viscosity from day to day to maintain a fixed Reynolds number throughout the entire series of measurements' (see p. 2 of the original paper).

and $$\Gamma = R_\vartheta^{1/4}\vartheta \left(\frac{q_1}{q_m}\right)^{-1/2} \frac{\mathrm{d}}{\mathrm{d}x}\left(\frac{q_1}{q_m}\right)^{1/2}, \quad (\vartheta \text{ and } x \text{ in foot}) \tag{6.7}$$

respectively.[1] The points marked with ● in FIGURES 7 and 8 were computed from the original table in this way.[2] Data undering these figures are shown collectively in TABLES 9 and 10 at the end of this note.

The followings will be remarked in both of these figures:

i) With respect to the functional form of $H(\Gamma)$ in the region of pressure rise, we notice that, as we go downstream along the surface of an obstacle, H_D (H-curve worked out from semi-empirical computations of VON DOENHOFF and TETERVIN) and H_S (H-curve constructed out of results of experimental work of SCHUBAUER and KLEBANOFF) have the same order of magnitude as, and run almost parallel with, H_H (H-curve proposed by HOWARTH making use of the data due to NIKURADSE and BURI) in the initial stage of their developments. However, after they have arrived at the definite values of Γ, each of the curves H_D and H_S changes its course suddenly and, instead of proceeding further, comes back to smaller values of $-\Gamma$ again, ascending very steeply to larger values of H at the same time. The most important feature of these curves is, therefore, that eventually $H_D(\Gamma)$ as well as $H_S(\Gamma)$ is no longer one-valued in the certain region of Γ; this is by no means acceptable for the assumptions underlying the differential equation (6.1). It is now very remarkable, by the way, that both of these curves behave quite similarly in the whole range of our discussion. This might be regarded as an indication for reliability of our present examination.

ii) Turning now to the functions $\zeta_D(\Gamma)$, $\zeta_S(\Gamma)$, and $\zeta_H(\Gamma)$ (as to the suffices D, S, and H, the same abbreviations as before have been used) differences quite considerable can be observed among these three functions. Namely ζ_D takes the values nearly constant, while ζ_S descends monotonically as we go from $\Gamma = 0$ down to -0.06. However, these two functions also are found two-valued: the curve of ζ_D comes backward making a very sharp angle at $\Gamma \simeq -0.04$ and ζ_S turns round gradually near $\Gamma = -0.06$. Besides, it should be noted that as we go downstream, the ζ_D-curve is found bending *upward* while the ζ_S-curve, *downward.* The point, or the value of $-\Gamma$, beyond which $H(\Gamma)$ and $\zeta(\Gamma)$ cease to be one-

1) In computing the derivative of $(q_1/q_m)^{1/2}$ with respect to x, the following formula has been used:

$$y_0' = \frac{1}{60h}(y_3 - 9y_2 + 45y_1 - 45y_{-1} + 9y_{-2} - y_{-3}),$$

cf. COLLATZ, L., *Numerische Behandlung von Differentialgleichungen* (1951), Anhang, Tafel III, S. 439. From the well-known property of numerical differentiation some error in the result should be expected inevitable. Scattering of points as observed in the curves of H_S and ζ_S, in the range of $0 > \Gamma > -0.02$ in particular, might be ascribed to this source of error.

2) VON DOENHOFF and TETERVIN calculated an example of retarding boundary layer, while on the other hand SCHUBAUER and KLEBANOFF measured the behaviors of the boundary layer, corresponding to the main stream first accelerated and next retarded. However, since we are now interested primarily in the region of pressure rise, only the second half of the their measurements were used as the material of our present investigation.

valued is common to both of these functions and moreover may not be regarded necessarily as the immediate neighborhood of the separation point.

To sum up: these two inquiries have shown that in a flow involving separation the functions $\zeta(\Gamma)$ as well as $H(\Gamma)$ can be regarded no longer as one-valued, which is by no means permissible for the calculation method due to HOWARTH. Thus the following questions are left for the future: 'These properties of Γ and H just revealed, are they confined to those two particular examples only, or generally valid for flows in boundary layers, or most generally for flows in boundary layers and in channes?' and further, 'How much accuracy can we expect in general from the approximation proposed by HOWARTH for computing boundary layers?'[1]

Appendix (laminar boundary layers)

The following computations are performed for laminar boundary layers, with a view to studying validities of law of velocity defects, of LUDWIEG-TILLMANN's power law for velocity profiles, together with of PRETSCH's formula, all of which were explained previously in connection with turbulent boundary layers as well as turbulent flows in channels (cf. (2.1), (2.2), (3.1), and (4.8)). To begin with, as an expression for velocity profiles, let us make use of the polynomial of VON KÁRMÁN and POHLHAUSEN.[2] Namely, denoting the velocity of the main stream just outside the laminar boundary layer by u_1 as before, we shall assume u, the x-component of the velocity, in the form

$$u/u_1 = F(\eta') + \Lambda G(\eta'),$$

where

$$F(\eta') = 2\eta' - 2\eta'^3 + \eta'^4, \quad G(\eta') = \eta'(1-\eta')^3/6, \tag{A.1}$$

$$\Lambda = \delta^2 du_1/\nu dx, \quad \text{and} \quad \eta' = y/\delta, \tag{A.2}$$ [3]

δ and x, y being thickness of the laminar boundary layer, and the coordinates measured along, and perpendicularly to, the wall.

By virtue of the polynomial approximation for velocity profiles, the displacement, and the momentum, thicknesses of a laminar boundary layer are readily given in the forms

$$\delta_1 = \frac{\delta}{120}(36-\Lambda),$$

and

$$\vartheta = \frac{\delta}{315}\left(37 - \frac{\Lambda}{3} - \frac{5\Lambda^2}{144}\right). \tag{A.3}$$

1) Concerning HOWARTH's approximate method, also see the following: OKABE, J., On the Tables of $u^{27/7}$ and $u^{-23/7}$, *Reports of Research Institute for Applied Mechanics*, vol. XII, no. 43 (1964), pp. 37-70, esp. 43-48.

2) GOLDSTEIN, S., *op. cit.*, vol. I (1938), **60**, p. 156 *et seq.*

3) η' is a quantity written usually as η; dash is attached in order to avoid confusions with η used already in section 4.

Λ takes the value -12 at the point of separation. Many investigations were published concerning so-called VON KÁRMÁN-POHLHAUSEN's method in which, for a given distribution of $u_1(x)$, Λ is computed as a function of x with the aid of the mementum equation, and it is found that the accuracy is not always satisfactory in the region of pressure rise and in particular near the separation. But, since we are now interested only in expressing the family of velocity profiles in terms of Λ, a form parameter, without correlating Λ with x actually, it is supposed that this procedure would yield the accuracy almost sufficient for our present purpose at least. The velocity profiles for six kinds of Λ, namely

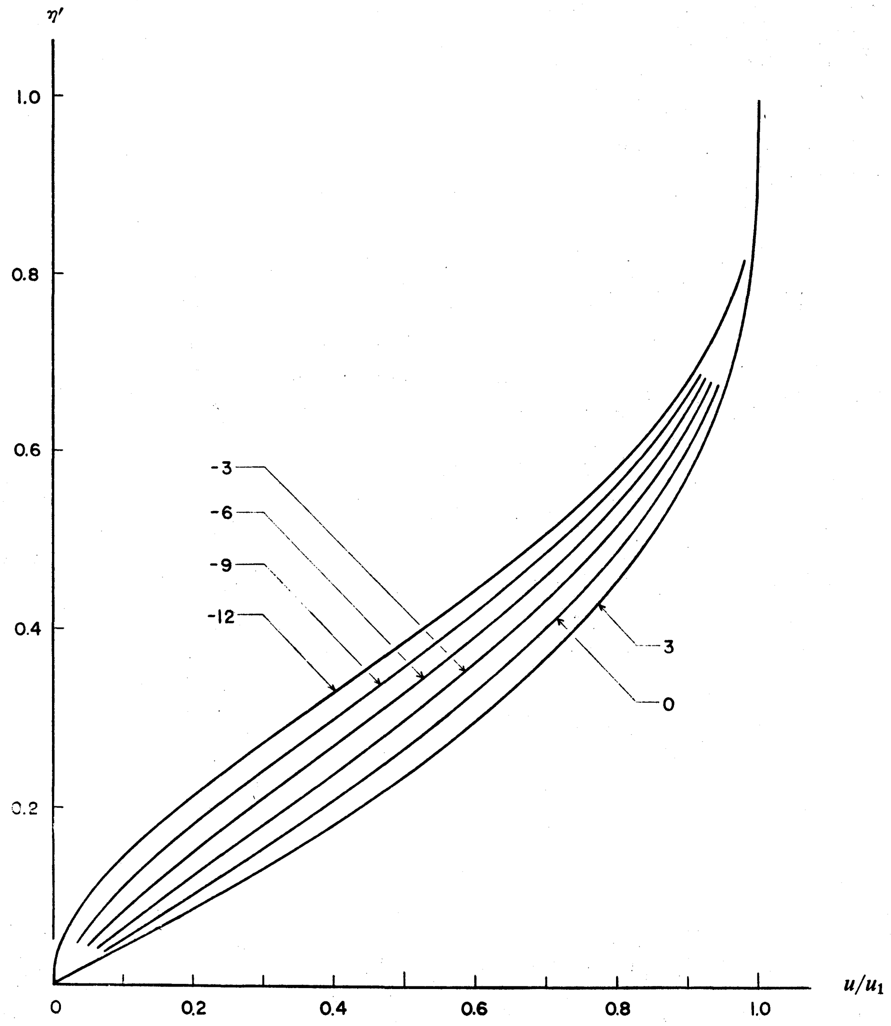

FIGURE A-1. Velocity profiles in laminar boundary layers.
The number attached to each curve denotes the corresponding value of Λ.

$$\Lambda = 3,\ 0,\ -3,\ -6,\ -9,\ \text{and}\ \ -12, \tag{A.4}$$

are reproduced in FIGURE A-1. Computations of values of δ_1/δ, ϑ/δ, and accordingly $H \equiv \delta_1/\vartheta$ for these values of Λ may be carried out easily and the results were shown already in TABLE 6.

Through this table, we are enabled to calculate values of η', $F(\eta')$, $G(\eta')$ and accordingly u/u_1 for various values of y/ϑ, and if therefore we define D_{lb}, the velocity defect in laminar boundary layers, corresponding to $\Lambda = \Lambda_*$ and $y/\vartheta = y_*/\vartheta$ by the equality

$$D_{lb} \equiv \frac{u}{u_1}\left(\Lambda_*, \frac{y_*}{\vartheta}\right) - \frac{u}{u_1}\left(0, \frac{y_*}{\vartheta}\right), \tag{A.5}$$

then we may evaluate D_{lb} as a function of y/ϑ for those values of Λ shown in (A.4). Result of this calculation is drawn as FIGURE A-2, and comparing it with FIGURE 1 in which velocity defects in turbulent boundary layer D_{tb} are given,

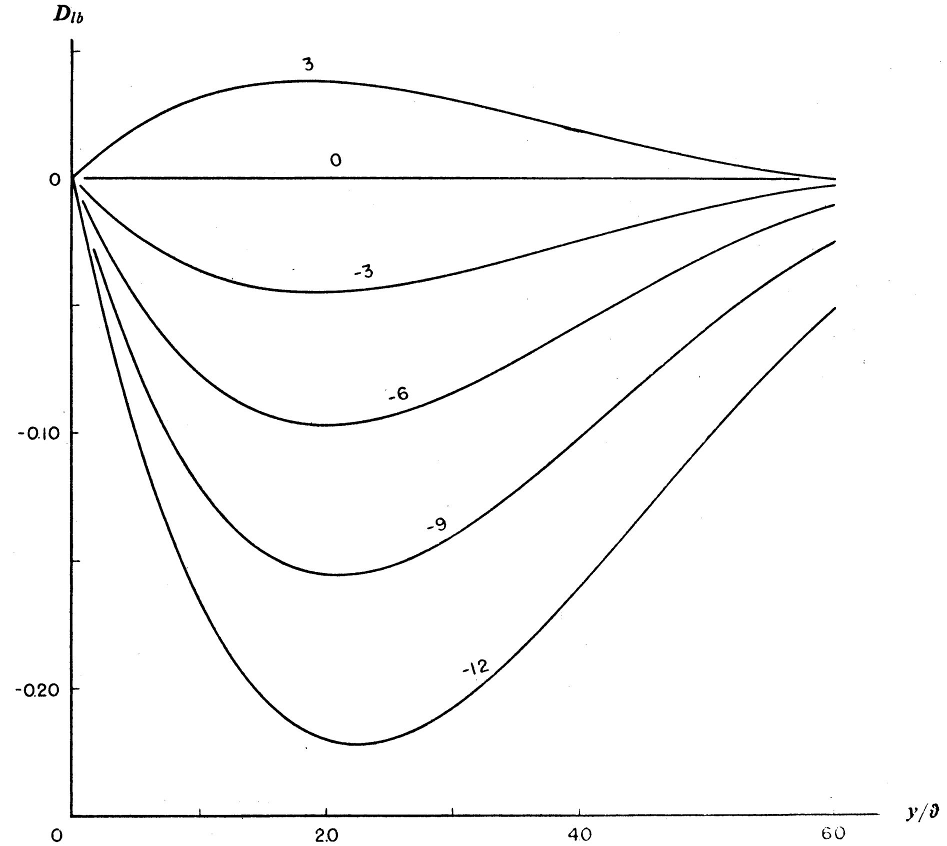

FIGURE A-2. Velocity defects in laminar boundary layers.
The number attached to each curve denotes the corresponding value of Λ.

we readily notice that, even for the velocity profiles of separation (defined by $H=2.7$ and by $\Lambda=-12$ for turbulent, and laminar, boundary layers respectively), the trough of D_{lb} is much shallower than that of D_{tb} and also that the value of

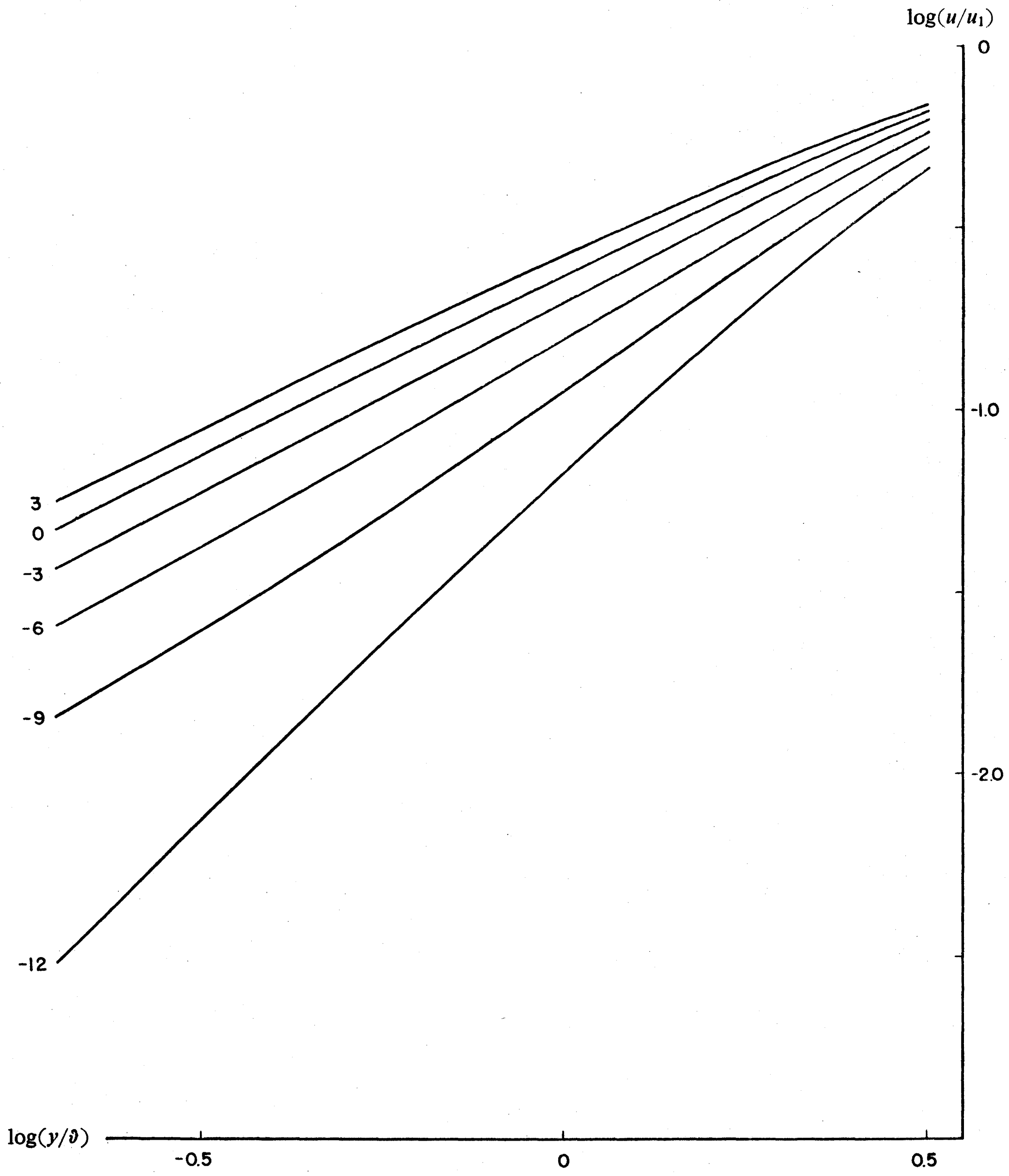

FIGURE A-3. LUDWIEG-TILLMANN's law in laminar boundary layers. The number attached to each curve denotes the corresponding value of Λ.

y/ϑ at which the maximum depression of the velocity defect is situated is found much larger in the laminar boundary layer than in the turbulent.

Next comes FIGURE A-3 which shows the relationship between $\log(u/u_1)$ and $\log(y/\vartheta)$ (log denotes common logarithm as before). In the region $y/\vartheta < 3$, approximately linear dependence will be observed between these quantities, the slope of the family of these straight lines, however, being of order 1, whereas in the case of turbulent boundary layers it was about 0.4.[1]

Lastly, the relationship between γ defined by (4.1) and H given in TABLE 6 was plotted with the mark ⊙ in FIGURE 5 (see p. 84). It is quite interesting to note that, except the velocity profile associated with separation, the functional form $\gamma(H)$ is almost similar to the cases of turbulent flows in boundary layers and in channels.

(Received January 13, 1965)

$\alpha = 4°$

y' cm	y'/b	y/b	τ/ρ cm/sec^2	τ/τ_0
2.6	0.960	0.040	70	2.333
2.4	0.890	0.110	140	4.667
2.2	0.815	0.185	204	6.800
2.0	0.740	0.260	256	8.533
1.8	0.670	0.330	290	9.667
1.6	0.590	0.410	313	10.433
1.4	0.520	0.480	326	10.867
1.2	0.445	0.555	328	10.933
1.0	0.370	0.630	325	10.833
0.8	0.300	0.700	290	9.667
0.6	0.22	0.78	230	7.667
0.4	0.15	0.85	160	5.333
0.2	0.075	0.925	80	2.667
0.1	0.037	0.963	40	1.333

$b = 2.70$ cm, $dp/\rho dx = 510$ cm/sec^2, $\tau_0/\rho = 30$ cm/sec^2.

TABLE 8-1.

---

1) Average values of those given in TABLES 2 and 4.

$\alpha = 3°$

y' cm	y'/b	y/b	τ/ρ cm/sec^2	τ/τ_0
2.0	0.930	0.070	150	2.000
1.8	0.840	0.160	230	3.067
1.6	0.740	0.260	294	3.920
1.4	0.650	0.350	340	4.533
1.2	0.560	0.440	360	4.800
1.0	0.465	0.535	360	4.800
0.8	0.370	0.630	332	4.427
0.6	0.280	0.720	284	3.787
0.4	0.186	0.814	200	2.667
0.2	0.093	0.907	100	1.333
0.1	0.047	0.953	50	0.667

$b = 2.15$ cm, $dp/\rho dx = 804$ cm/sec^2, $\tau_0/\rho = 75$ cm/sec^2.

TABLE 8–2.

$\alpha = 2°$

y' cm	y'/b	y/b	τ/ρ cm/sec^2	τ/τ_0
1.6	0.97	0.03	190	1.267
1.5	0.91	0.09	250	1.667
1.4	0.85	0.15	300	2.000
1.2	0.73	0.27	370	2.467
1.0	0.61	0.39	380	2.533
0.8	0.49	0.51	368	2.453
0.6	0.37	0.63	330	2.200
0.4	0.24	0.76	240	1.600
0.2	0.12	0.88	130	0.867
0.1	0.06	0.94	65	0.433
0.05	0.03	0.97	33	0.220

$b = 1.65$ cm, $dp/\rho dx = 1085$ cm/sec^2, $\tau_0/\rho = 150$ cm/sec^2.

TABLE 8–3.

$\alpha = 1°$

y' cm	y'/b	y/b	τ/ρ cm/sec^2	τ/τ_0
1.0	0.91	0.09	390	1.258
0.9	0.82	0.18	425	1.371
0.8	0.73	0.27	445	1.435
0.7	0.64	0.36	445	1.435
0.6	0.55	0.45	430	1.387
0.5	0.45	0.55	395	1.274
0.4	0.36	0.64	338	1.090
0.3	0.27	0.73	270	0.871
0.2	0.18	0.82	190	0.613
0.1	0.09	0.91	100	0.323
0.05	0.046	0.954	50	0.161

$b = 1.10$ cm, $dp/\rho dx = 1725$ cm/sec^2, $\tau_0/\rho = 310$ cm/sec^2.

TABLE 8-4.

$\alpha = 0°$

y' cm	y'/b	y/b	τ/ρ cm/sec^2	τ/τ_0
0.55	0.92	0.08	890	0.917
0.50	0.83	0.17	810	0.834
0.45	0.75	0.25	730	0.752
0.40	0.67	0.33	650	0.669
0.35	0.58	0.42	568	0.585
0.30	0.50	0.50	488	0.503
0.25	0.42	0.58	408	0.420
0.20	0.33	0.67	325	0.335
0.15	0.25	0.75	245	0.252
0.10	0.17	0.83	168	0.173
0.05	0.08	0.92	85	0.088
0.025	0.04	0.96	44	0.045

$b = 0.60$ cm, $dp/\rho dx = -1630$ cm/sec^2, $\tau_0/\rho = 971$ cm/sec^2.

TABLE 8-5.

$\alpha = -2°$

y' cm	y'/b	y/b	τ/ρ cm/sec²	τ/τ_0
0.95	0.93	0.07	330	0.880
0.90	0.88	0.12	280	0.747
0.80	0.79	0.21	110	0.293
0.70	0.69	0.31	56	0.149
0.60	0.59	0.41	30	0.080
0.40	0.39	0.61	10	0.027
0.30	0.30	0.70	5.7	0.015
0.20	0.20	0.80	3.0	0.008

$b = 1.02$ cm, $dp/\rho dx = -5460$ cm/sec², $\tau_0/\rho = 375$ cm/sec².

TABLE 8-6.

$\alpha = -4°$

y' cm	y'/b	y/b	τ/ρ cm/sec²	τ/τ_0
1.40	0.97	0.03	140	0.636
1.35	0.94	0.06	110	0.500
1.30	0.90	0.10	70	0.318
1.20	0.83	0.17	27	0.123
1.1	0.76	0.24	12	0.055
1.0	0.69	0.31	5	0.023

$b = 1.44$ cm, $dp/\rho dx = -3730$ cm/sec², $\tau_0/\rho = 220$ cm/sec².

TABLE 8-7.

$\alpha = -8°$

y' cm	y'/b	y/b	τ/ρ cm/sec²	τ/τ_0
2.2	0.97	0.03	27	0.284
2.1	0.92	0.08	19	0.200
2.0	0.88	0.12	11	0.116
1.9	0.83	0.17	6	0.063
1.8	0.79	0.21	2	0.021

$b = 2.28$ cm, $dp/\rho dx = -1830$ cm/sec², $\tau_0/\rho = 95$ cm/sec².

TABLE 8-8.

x/c	$-\Gamma\times10^2$	H	$\zeta\times10^2$
0.075	0.196	1.564	1.271
085	201	558	271
125	224	537	281
135	235	535	281
150	251	528	280
0.165	0.268	1.526	1.286
200	315	523	290
220	338	523	293
250	360	524	297
300	392	528	305
0.350	0.557	1.533	1.310
360	0.618	536	312
380	0.756	543	315
400	0.939	553	320
420	1.152	567	323
0.430	1.290	1.578	1.326
440	1.438	589	325
450	1.629	602	330
460	1.834	617	326
470	2.059	635	331
0.475	2.185	1.646	1.331
480	333	658	336
485	477	671	336
490	642	686	338
495	828	702	337
0.500	3.023	1.721	1.342
505	201	742	342
510	384	766	342
515	563	794	345
520	756	826	346
0.525	3.953	1.865	1.349
530	4.142	1.912	350
535	4.166	1.971	349
540	3.641	2.045	355
545	3.375	2.126	357
0.550	3.103	2.225	1.357
555	2.839	349	358
560	2.603	511	359
565		735	

TABLE 9.

x ft	$-\Gamma\times10^2$	H	$\zeta\times10^2$
14.5	0.059	1.33	2.331
15.5	-0.004	38	2.235
16.5	-0.060	34	2.165
17.5	0.039	35	2.018
18.0	0.388	37	1.936
18.5	0.863	1.31	1.935
19.0	1.233	37	1.870
19.5	1.320	33	1.808
20.0	1.524	40	1.721
20.5	1.759	45	1.664
21.0	1.923	1.49	1.594
21.5	2.714	47	1.502
22.0	3.408	54	1.401
22.5	3.925	60	1.324
23.0	4.476	65	1.191
23.5	4.965	1.75	1.022
24.0	5.882	1.87	0.761
24.5	6.070	1.99	0.349
*25.0	4.955	2.18	0.119
*25.5	3.780	2.48	0.000
*26.0	3.228	3.22	0.000

Data added with an asterisk were obtained by modifying or extrapolating the values of δ_1 and ϑ given in the original paper.

TABLE 10.